



**SOUTHERN PLAINS**  
TRANSPORTATION CENTER

## **Evaluation of Surface Treatments to Mitigate ASR**

Matthew Waidner  
Richard Deschenes, Jr., Ph.D.  
W. Micah Hale, Ph.D., P.E.

**SPTC14.1-20-F**

**Southern Plains Transportation Center  
201 Stephenson Parkway, Suite 4200  
The University of Oklahoma  
Norman, Oklahoma 73019**

*DISCLAIMER*

*The contents of this report reflect the views of the authors, who are responsible for the facts and accuracy of the information presented herein. This document is disseminated under the sponsorship of the Department of Transportation University Transportation Centers Program, in the interest of information exchange. The U.S. Government assumes no liability for the contents or use thereof.*

1. Report No. SPTC14.1-20-F	2. Government Accession No.	3. Recipient's Catalog No.	
4. Title and Subtitle  Evaluation of Surface Treatments to Mitigate ASR		5. Report Date December 2019	
		6. Performing Organization Code	
7. Authors  Matthew Waidner, Richard Deschenes, Jr., and W. Micah Hale		8. Performing Organization Report No.	
9. Performing Organization Name and Address Department of Civil Engineering University of Arkansas 4190 Bell Fayetteville, AR 72701		10. Work Unit No. (TRAIS)	
		11. Contract or Grant No.  DTRT13-G-UTC36	
12. Sponsoring Agency Name and Address  Southern Plains Transportation Center 201 Stephenson Pkwy, Suite 4200 The University of Oklahoma Norman, OK 73019		13. Type of Report and Period Covered  Final Report, July 2014 – December 2019	
		14. Sponsoring Agency Code	
15. Supplementary Notes  University Transportation Center			
16. Abstract  Premature cracking of the barrier wall and pavement on I-49 south of Fayetteville, Arkansas due to a combination of Alkali-Silica Reaction (ASR) and freeze-thaw has led to ASR and freeze-thaw research at the University of Arkansas. Potential for further expansion (PFET), Damage Rating Index (DRI), and mitigation of freeze-thaw and ASR with sealers testing and results are contained herein. PFET results indicated that the pavement will not continue to expand from ASR. With other interstate pavements deteriorating prematurely throughout Arkansas, DRI has shown that most are damaged not only by ASR but by freeze-thaw too. Recommendations for freeze-thaw's inclusion into DRI are included. Results for a sealer that will limit ASR and freeze-thaw expansion are given and have shown that silanes with 40% silane work effectively to reduce ASR and freeze-thaw expansion.			
17. Key Words Alkali silica reaction, freeze and thawing, mitigation	18. Distribution Statement  No restrictions. This publication is available at <a href="http://www.sptc.org">www.sptc.org</a> and from the NTIS.		
19. Security Classif. (of this report)  UNCLASSIFIED	20. Security Class. (of this page)  UNCLASSIFIED	21. No. of Pages  88	22. Price

# SI\* (MODERN METRIC) CONVERSION FACTORS

## APPROXIMATE CONVERSIONS TO SI UNITS

SYMBOL	WHEN YOU KNOW	MULTIPLY BY	TO FIND	SYMBOL
<b>LENGTH</b>				
in	inches	25.4	millimeters	mm
ft	feet	0.305	meters	m
yd	yards	0.914	meters	m
mi	miles	1.61	kilometers	km
<b>AREA</b>				
in <sup>2</sup>	square inches	645.2	square millimeters	mm <sup>2</sup>
ft <sup>2</sup>	square feet	0.093	square meters	m <sup>2</sup>
yd <sup>2</sup>	square yard	0.836	square meters	m <sup>2</sup>
ac	acres	0.405	hectares	ha
mi <sup>2</sup>	square miles	2.59	square kilometers	km <sup>2</sup>
<b>VOLUME</b>				
fl oz	fluid ounces	29.57	milliliters	mL
gal	gallons	3.785	liters	L
ft <sup>3</sup>	cubic feet	0.028	cubic meters	m <sup>3</sup>
yd <sup>3</sup>	cubic yards	0.765	cubic meters	m <sup>3</sup>
NOTE: volumes greater than 1000 L shall be shown in m <sup>3</sup>				
<b>MASS</b>				
oz	ounces	28.35	grams	g
lb	pounds	0.454	kilograms	kg
T	short tons (2000 lb)	0.907	megagrams (or "metric ton")	Mg (or "t")
<b>TEMPERATURE (exact degrees)</b>				
°F	Fahrenheit	5 (F-32)/9 or (F-32)/1.8	Celsius	°C
<b>ILLUMINATION</b>				
fc	foot-candles	10.76	lux	lx
fl	foot-Lamberts	3.426	candela/m <sup>2</sup>	cd/m <sup>2</sup>
<b>FORCE and PRESSURE or STRESS</b>				
lbf	poundforce	4.45	newtons	N
lbf/in <sup>2</sup>	poundforce per square inch	6.89	kilopascals	kPa
<b>APPROXIMATE CONVERSIONS FROM SI UNITS</b>				
SYMBOL	WHEN YOU KNOW	MULTIPLY BY	TO FIND	SYMBOL
<b>LENGTH</b>				
mm	millimeters	0.039	inches	in
m	meters	3.28	feet	ft
m	meters	1.09	yards	yd
km	kilometers	0.621	miles	mi
<b>AREA</b>				
mm <sup>2</sup>	square millimeters	0.0016	square inches	in <sup>2</sup>
m <sup>2</sup>	square meters	10.764	square feet	ft <sup>2</sup>
m <sup>2</sup>	square meters	1.195	square yards	yd <sup>2</sup>
ha	hectares	2.47	acres	ac
km <sup>2</sup>	square kilometers	0.386	square miles	mi <sup>2</sup>
<b>VOLUME</b>				
mL	milliliters	0.034	fluid ounces	fl oz
L	liters	0.264	gallons	gal
m <sup>3</sup>	cubic meters	35.314	cubic feet	ft <sup>3</sup>
m <sup>3</sup>	cubic meters	1.307	cubic yards	yd <sup>3</sup>
<b>MASS</b>				
g	grams	0.035	ounces	oz
kg	kilograms	2.202	pounds	lb
Mg (or "t")	megagrams (or "metric ton")	1.103	short tons (2000 lb)	T
<b>TEMPERATURE (exact degrees)</b>				
°C	Celsius	1.8C+32	Fahrenheit	°F
<b>ILLUMINATION</b>				
lx	lux	0.0929	foot-candles	fc
cd/m <sup>2</sup>	candela/m <sup>2</sup>	0.2919	foot-Lamberts	fl
<b>FORCE and PRESSURE or STRESS</b>				
N	newtons	0.225	poundforce	lbf
kPa	kilopascals	0.145	poundforce per square inch	lbf/in <sup>2</sup>

\*SI is the symbol for the International System of Units. Appropriate rounding should be made to comply with Section 4 of ASTM E380.

**EVALUATION OF SURFACE TREATMENTS  
TO MITIGATE ASR**

**Final Report**

**December 2019**

**Matthew Waidner, Structural Engineer**, Tatum, Smith, Welcher, Rogers, AR  
**Richard Deschenes, Jr., Ph.D., Assistant Professor**, Youngstown State University,  
Youngstown, OH  
**W. Micah Hale, Ph.D., P.E., Professor**, University of Arkansas, Fayetteville, AR

**Southern Plains Transportation Center  
201 Stephenson Parkway, Suite 4200  
The University of Oklahoma  
Norman, Oklahoma 73019**

## **Table of Contents**

1	Introduction and Background .....	1
2	Literature Review.....	3
2.1	Alkali-Silica Reaction (ASR) .....	3
2.2	Test Methods for Determining ASR .....	5
2.2.1	Aggregate Reactivity .....	5
2.2.1.1	ASTM C 227 (MBT) .....	5
2.2.1.2	ASTM C 1260 (AMBT).....	6
2.2.1.3	ASTM C 1293 (CPT).....	7
2.2.2	Hardened Concrete.....	7
2.2.2.1	Potential for Further Expansion .....	7
2.2.2.2	Visual Inspection .....	9
2.3	Monitoring .....	11
2.3.1	Expansion Readings.....	11
2.3.2	Cracking Index.....	11
2.4	Prevention of ASR .....	12
2.5	Mitigation of ASR.....	14
2.6	Freeze-Thaw .....	16
2.7	Test Methods for Determining Freeze-Thaw.....	19
2.7.1	Aggregate Susceptibility .....	19
2.7.1.1	AASHTO T 104/ASTM C 88 (Sulfate Soundness) .....	19
2.7.1.2	AASHTO T 161/ASTM C 666 (Rapid Freezing and Thawing) .....	20
2.7.2	Visual Inspection .....	21
2.7.2.1	Petrography .....	21
2.8	Prevention of Freeze-Thaw.....	21
2.9	Mitigation of Freeze-Thaw .....	22
2.10	Purpose of Research.....	23
3	Methods and Materials.....	25
3.1	Experimental Program .....	25
3.2	Damage Rating Index (DRI) .....	25
3.3	Potential for Further Expansion Test .....	30
3.4	ASR and Freeze-Thaw Mitigation by Sealers .....	34
4	Results.....	40
4.1	Experimental Program .....	40
4.2	Damage Rating Index .....	40
4.2.1	I-530 Pavement .....	41
4.2.2	I-30 Pavement .....	46
4.2.3	I-49 Pavement .....	47
4.2.4	Joint and Mid Slab .....	50
4.3	Potential for Further Expansion Test.....	53
4.4	ASR and Freeze-Thaw Mitigation by Sealers .....	53
5	Recommendations and Conclusions .....	69
5.1	Recommendations and Conclusions from DRI.....	69
5.2	Conclusions from the Potential for Further Expansion Test.....	70
5.3	Conclusions from Mitigation .....	71
6	References.....	73

Appendix A.....	76
-----------------	----

## **List of Tables**

Table 2.1 Reactive Siliceous Materials .....	4
Table 2.2 Grattan-Bellew DRI Feature and Factor 1992 .....	11
Table 2.3 Sanchez DRI Feature and Factor 2014 .....	11
Table 3.1 Grit Times .....	26
Table 3.2 Petrographic features and weighing factors .....	30
Table 3.3 Mix Design Group 1 .....	35
Table 3.4 Mix Design Group 2 .....	36
Table 3.5 Treatments Group 1 .....	38
Table 3.6 Treatments Group 2 .....	39
Table 3.7 Chemical Compositions of Treatments .....	40
Table 4.1 Labeling Convention .....	42
Table 4.2 DRI Feature Abbreviations .....	43
Table 4.3 Control Blocks Overall Expansion Group 1 .....	55
Table 4.4 Linseed Oil Overall Expansion Group 1 .....	57
Table 4.5 Silane Overall Expansion Group 1 .....	58
Table 4.6 Percent Change Group 1 .....	58
Table 4.7 Control Blocks Overall Expansion Group 2 .....	60
Table 4.8 Silane Blocks Overall Expansion Group 2 .....	61
Table 4.9 Linseed Oil Overall Expansion Group 2 .....	62
Table 4.10 Lithium Overall Expansion Group 2 .....	64
Table 4.11 Percent Change Group 2 .....	64
Table 4.12 Concrete Temperature 1.5 in Below Surface .....	66
Table 4.13 Concrete Temperature 3 in Below Surface .....	67
Table 4.14 Average Concrete Temperature Data .....	67



## **List of Figures**

Figure 3.1 Polishing Patterns .....	28
Figure 3.2 Bucket with Cores over Water .....	31
Figure 3.3 Water Bath.....	33
Figure 3.4 Length Change Comparator .....	34
Figure 3.5 Formwork .....	37
Figure 4.1 I-530 DRI .....	44
Figure 4.2 I-530 Feature Count.....	45
Figure 4.3 I-30 DRI.....	46
Figure 4.4 I-30 Feature Count.....	46
Figure 4.5 I-49 DRI.....	47
Figure 4.6 I-49 Feature Count.....	48
Figure 4.7 An “Exploded” Aggregate.....	49
Figure 4.8 Mid Slab DRI .....	50
Figure 4.9 Joint DRI .....	51
Figure 4.10 Mid Slab Feature Count.....	51
Figure 4.11 Joint Feature Count.....	52
Figure 4.12 PFET on I-49 .....	53
Figure 4.13 Control Blocks Strain Group 1 .....	55
Figure 4.14 Linseed Oil Strain N-S Group 1 .....	56
Figure 4.15 Linseed Oil Strain E-W Group 1 .....	56
Figure 4.16 Silane Strain N-S Group 1 .....	57
Figure 4.17 Silane Strain E-W Group 1 .....	58
Figure 4.18 Control Blocks Strain Group 2 .....	59
Figure 4.19 Silane Blocks Strain N-S Group 2.....	60
Figure 4.20 Silane Blocks Strain E-W Group 2.....	61
Figure 4.21 Linseed Oil Strain Group 2.....	62
Figure 4.22 Lithium Strain N-S Group 2 .....	63
Figure 4.23 Lithium Strain E-W Group 2 .....	63

## **Executive Summary**

Premature cracking of the barrier wall and pavement on I-49 south of Fayetteville, Arkansas due to a combination of Alkali-Silica Reaction (ASR) and freeze-thaw has led to ASR and freeze-thaw research at the University of Arkansas. Potential for further expansion (PFET), Damage Rating Index (DRI), and mitigation of freeze-thaw and ASR with sealers testing and results are contained herein. PFET results indicated that the pavement will not continue to expand from ASR. With other interstate pavements deteriorating prematurely throughout Arkansas, DRI has shown that most are damaged not only by ASR but by freeze-thaw too. Recommendations for freeze-thaw's inclusion into DRI are included. Results for a sealer that will limit ASR and freeze-thaw expansion are given and have shown that silanes with 40% silane work effectively to reduce ASR and freeze-thaw expansion.

## **1 Introduction**

In 2012 the barrier wall and pavement along I-49 was seen to be undergoing premature deterioration. The Arkansas Highway and Transportation Department (AHTD) took concrete samples from both for petrographic examination. The results of the examination indicated that Alkali-Silica Reaction (ASR) and freeze-thaw had caused deterioration in the concretes.

A research program starting in May 2012 by the University of Arkansas has been monitoring the barrier wall and pavement along I-49. Monitoring has revealed that the barrier wall and pavement are still expanding and cracking. This has led the program to take new cores in June 2014 for an ASR potential expansion test to see how much more the pavement will expand.

Since 2012, I-30 in Little Rock and I-530 around Pine Bluff have shown signs of ASR and freeze-thaw causing premature deterioration. With the addition of other concrete pavements experiencing distress due to ASR and freeze-thaw, there has been interest in using the Damage Rating Index (DRI) to quantify the damage of these pavements, and then determine the appropriate mitigation method (Gratten-Bellew 1992).

While ASR is believed to be the original cause of the deterioration in the I-49 concrete, freeze-thaw cracking has assisted in bolstering the deterioration (Deschenes 2014). The past several winters (2011-2015) have brought more than the average snow and icefall for Arkansas and the I-49 pavement has shown an increase in D-cracking due to these winters. The goal of the author's research now is to find a sealer that will mitigate ASR while also being resistant to these freeze-thaw cycles.

DRI counts and potential expansion data have been prepared in this paper. Their recommendations and conclusions are provided. The preliminary results of the sealants test have been also prepared in this paper. However, the current data shown is only for a year and three

months. Five to seven years of testing are recommended for determining an appropriate sealant. Recommendations and conclusions are still provided on the preliminary results of the sealants test.

## 2 Literature Review

### 2.1 Alkali-Silica Reaction

Alkali-Silica Reaction (ASR) occurs in concrete when the alkalis in the cement react with the silica in the aggregates. The result of the reaction is the formation of an alkali-silica gel. When this gel comes into contact with water it expands creating pressure within the concrete matrix. Once the pressure exceeds the tensile strength of the concrete, cracking starts.

ASR was discovered by Thomas Stanton in 1940, when asked to determine the cause of early cracking in the King City Bridge in California. Stanton learned that a local fine aggregate was reacting with the high-alkali cement used in the bridge. After testing different combinations of cements, with varying alkali contents, and aggregates using the mortar bar test, Stanton determined that only siliceous rocks reacted with cements. He also determined that cements with an alkali content greater than 0.6 percent reacted with the aggregates (Stanton 1940).

Stanton developed a formula to calculate the available equivalent alkalis in cement. Equivalent alkalis are  $\text{Na}_2\text{O}$  and  $\text{K}_2\text{O}$ . The equation is the percent of  $\text{Na}_2\text{O} + 0.658(\text{K}_2\text{O})$  (Stanton 1940). These alkalis produce a high amount of hydroxyl ions that react with the silica. The result of the reaction is an alkali rich gel (Lute 2008). However, when the equivalent alkalis are kept below 0.6%, the hydroxyl content is too low to produce enough alkali rich gel to cause significant expansion (Stanton 1940).

However, not all aggregates that contain silica are reactive with alkalis. The silica in the aggregate must be soluble in high pH concrete pore solution. Also, the crystalline structure of the silica must break down to react with the hydroxyl ions (Folliard 2006). Silica with amorphous, disordered, or poor crystalline structures will react with hydroxyl ions (Lute 2008). Table 2.1 provides a list of reactive aggregates and minerals (Folliard 2006).

Table 2.1. Reactive Siliceous Materials

Reactive Siliceous Materials	
Aggregate Types	Minerals
Arenite, Argillite, Arkose, Chert, Flint, Gneiss, Granite, Greywacke, Hornfels, Quartz-Arenite, Quartzite, Sandstone, Shale, Silicified Carbonate, and Siltstone	Crisobalite, Cryptocrystalline Quartz Opal, Strained Quartz Tridymite, and Volcanic Glass

Much research has been conducted on determining which aggregates are reactive; however, there are many aggregates whose reactivity is still not known. This is because over time silica content in the aggregate changes. Also, testing aggregate from many quarries across the United States is time consuming and expensive.

In order for the reaction to continue after cement hydration, there must be sufficient moisture in the concrete. The amount of moisture in concrete is measured as relative humidity. In 1991, Stark determined that there must be at least 80 percent relative humidity in concrete for ASR to continue. He also learned that in most climate exposures, including arid deserts, concrete can maintain a relative humidity above 80 percent (Stark 1991). The moisture can come from rain, rivers, seawater, mix water, or any source of water.

Moderate temperatures can reduce the relative humidity of concrete to below 80 percent (Stark 1991b). However, the higher the temperature the faster the reaction takes place (ACI221 1998). Generally, this occurs during the summer after a rainstorm, when the sun comes out. The rain provides enough moisture to start the reaction and cause ASR gel to swell, while the increased temperature increases the rate of the reaction.

Since moisture is a key component of ASR formation, reducing the permeability of the concrete will prevent the potential for expansion. Lowering the permeability of concrete can be achieved by lowering the water-cement ratio, by adding mineral admixtures, such as fly ash or silica fume, or by adequate curing (Durand and Chen 1991).

## 2.2 Test Methods for Determining ASR

There are many test methods for determining if ASR is going to or is causing deterioration in concrete. Test methods can be divided up into four main groups: Aggregate Reactivity, Hardened Concrete, Visual Inspection, and Monitoring.

### 2.2.1 Aggregate Reactivity

#### 2.2.1.1 ASTM C 227 (MBT)

The Mortar-Bar Expansion Test (MBT) is described in ASTM C 227. The purpose of the test is to determine if the selected aggregate is reactive with the cement in a mortar mixture. The cement should have at least 0.6% equivalent alkalis. ASTM C 227 provides the specific gradation that the aggregate must meet whether it is a fine or coarse aggregate. Four mortar bars are fabricated from two batches of the same mix. The bars are demolded after one day and measured lengthwise in a comparator for the initial reading. They are then placed into containers lined with wick and over an inch of water. The containers are then sealed and placed into a chamber kept at 38°C. These conditions provide a 100 percent relative humidity environment for the mortar bars. This condition will accelerate ASR in the mortar bars, if the aggregate is reactive.

The mortars bars are to be measured at days 1 and 14, and months 1, 2, 3, 4, 5, and 6 (ACI 221 1998). Prior to measuring length change the containers are removed from the chamber and allowed to cool to 23°C for at least 16 hours. The mortar bars are then extracted from the containers and placed in the comparator to obtain a strain reading. After each mortar bar is measured, they are placed back in their containers and into the chamber. After 6 months of readings, if the average expansion greater than 0.1%, then the aggregate is considered potentially deleterious (ASTM C 33-16).

However, ASTM C 227 gives a warning that using the MBT alone does not provide enough information if the aggregate is reactive, though the MBT is considered one of the most accurate indicators if an aggregate is reactive. It is suggested that the use of other tests in combination with the MBT will best help determine if an aggregate is truly reactive. This is because the MBT assumes that all aggregates react the same way to produce ASR. It is known that some reactive aggregates expand slowly and when given enough time will exceed the 0.1% expansion mark after 6 months.

#### 2.2.1.2 ASTM C 1260 (AMBT)

The Accelerated Mortar-Bar Test (AMBT) is described in ASTM C 1260. The AMBT is a modification of the MBT and also is used to determine if an aggregate is reactive. The mixture proportions and container set-up are the same as the MBT. However, the containers are filled with a 1N NaOH solution, which the mortar bars are submerged in, and the chamber or water bath temperature is increased to 80°C. These new conditions accelerate any reaction because of the increase in alkalis from the NaOH and increase in temperature.

Length change of the mortar bars is measured at days 1 and 14, and three other intermediate readings. When it is time to take a reading, the readings need to be taken within 10 minutes to ensure that the temperature of the mortar bars does not drop low enough to slow the reaction. After 14 days, if the average expansion is over 0.1% but less than 0.2%, then the aggregate will be considered innocuous and deleterious. If the average expansion is above 0.2%, then the aggregate will be considered potentially reactive (ASTM C 33-16).

ASTM C 1260 warns that the AMBT alone does not ensure that an aggregate is reactive. This is evident in the 0.1% to 0.2% expansion range, a gray area, where the aggregate is considered both unreactive and reactive. Tests like the MBT or the Concrete Prism Test (CPT)



may help determine if the aggregate is truly reactive. Also, the increase in alkalis and in temperature may cause some aggregates to be reactive, when in the field they are generally unreactive with less alkalis. Overall, however, the AMBT is good at finding reactive aggregates that are slow reacting.

#### 2.2.1.3 ASTM C 1293 (CPT)

The Concrete Prism Test (CPT) is described in ASTM C 1293. The CPT is used to determine aggregate reactivity in a concrete mixture whereas the previous tests only examined mortar mixtures. The aggregate preparations and container set-up are similar to the MBT. The cement must have at least a 0.9% equivalent alkali content, and extra NaOH is added to the mix water to increase the equivalent alkali content to 1.25% by mass of cement.

Length change of the concrete specimens is measured at days 1, 7, 18, and 56, and months 3, 6, 9, and 12. Before each reading the prisms are cooled to 23°C for at least 16 hours. After 1 year of readings, if the average expansion is greater than 0.04%, then the aggregate is considered potentially deleteriously reactive (ASTM C 33-16).

However, the CPT alone does not always indicate whether an aggregate is truly reactive. The CPT, like the MBT, assumes all aggregates react the same way, but some aggregates react slower and may be considered unreactive, when if given enough time will cause expansions greater than 0.04%.

### 2.2.2 Hardened Concrete

#### 2.2.2.1 Potential for Further Expansion

The only test that has been proven to work for determining ASR reactivity in hardened concrete is the Potential for Further Expansion Test (PFET). The PFET was developed by Stark in 1991 and is a combination of the AMBT and CPT. Cores are taken from the concrete

structure that is suspected of having ASR. At least nine cores are needed for the test and each is fitted with gage studs in the ends to measure length change in a comparator. The cores are split evenly between the following containers. One container is lined with wick and 1 inch of water is placed at the bottom of the container. This container will provide a humid environment for the cores. Another container is filled with water that is at room temperature. The cores submerged in water will be used to measure the amount of expansion due to water intake. The final container is filled with 1N NaOH solution. Cores submerged in the 1N NaOH solution will have an unlimited supply of alkalis to promote ASR. The 1N NaOH solution should be changed after 6 months to ensure those cores continue to have enough alkalis. The containers are placed into a water bath with a temperature of 38°C (Stark 1991a).

Measurements are taken on the cores every week for one year. Before each reading, the containers are removed from the water bath for at least 16 hours to cool to 23°C. After one year of measurements, it is noted whether the cores have expanded over 1 inch of water. If they have expanded, then there is a sufficient amount of alkalis in the concrete for ASR to continue. After subtracting the expansion of the core submerged in water from the 1N NaOH cores, if that expansion is greater than 0.03%, then there is a sufficient amount reactive silica left in the concrete for ASR to continue. Both criteria must be met for ASR to continue in the concrete (Stark 1991a).

The test does have problems due to alkali leaching of the concrete into solution. Alkali leaching causes ASR to stop within the concrete and can give lower expansion results than would actually happen without alkali leaching. Therefore to prevent alkali leaching, it is important to replace the 1N NaOH solution at least every 6 months. Another problem is that while the test can conclude that the concrete will not expand anymore due to limited alkalis, it

does not take into account that alkalis can come from other sources such as deicing salts on concrete pavements.

#### 2.2.2.2 Visual Inspection

Visual inspection or petrography can be used to determine if ASR is the cause for concrete deterioration. Visible inspection of the concrete pavement that is affected by ASR will show signs of map cracking, gel extruding from cracks, and joints crushing.

Cracking that appears on the concrete surface caused by ASR generally occur in a jagged polygon manner and is referred to as “map cracking.” This cracking does not extend deeper than 300 to 400mm (ACI221 1998). ASR gel that is extruding from cracks is another sign of ASR. The use of uranyl acetate applied to the gel and examination of the gel under UV light will determine if the gel is ASR gel or not. The gel will turn purple under UV light once the uranyl acetate is applied. The final visible feature that is common with ASR is joints crushing. As expansion of the concrete continues joints in the pavement will close. After the joint has closed, pressure from expansion starts to build until the joint either pops up or it slowly crushes.

Petrography is another way to determine if ASR is the cause of concrete deterioration. Concrete cores are removed from the pavement. A petrographer will cut and polish the cores into thin sections to examine them under a microscope. Then, a couple different methods can be used to determine if ASR is the cause.

First, as stated before, uranyl acetate can be used along with a UV light to determine the presence of ASR. Second, the cracking pattern and presence of reaction rims can indicate ASR deterioration. Once ASR has been confirmed in the concrete, then it is important to determine the amount of damage already present. This can be done using the visual inspection and petrography combined with a damage rating index (DRI).

The damage rating index was developed by Grattan-Bellew in 1992. Cores are taken from the pavement and sawn in two down the length of the core. Each half is polished and then a grid of 1 cm by 1 cm squares is drawn on the core. A microscope with 16x magnification is used to examine each half for features characteristic of ASR. The tables of features are shown in Table 2.2 and Table 2.3. Since Grattan-Bellew's first feature and factor list, several features have been removed and added. Reaction rims and air voids lined with gel were removed because they did not signify actual damage in the concrete. Disaggregated/corroded aggregate particles was added since some aggregate particles were disintegrated to the point where cracks could no longer be counted, yet the aggregate was obviously damaged. Opened cracks or network of cracks in coarse aggregate particle was added to distinguish from closed cracks in the aggregate particle, since an open crack or network of cracks is a sign of greater damage (Grattan-Bellew 1992 and Sanchez 2014).

Each 1 cm by 1 cm square is examined individually and the features that are in the square are counted and the factor is applied. At least 200 cm<sup>2</sup> should be examined from each core to give an accurate DRI number that describes the damage of the concrete. The final DRI number is normalized to 100 cm<sup>2</sup> (Sanchez 2014). DRI numbers are used to characterize the damage. DRI's from 0 to 350 are slightly damaged, 350-600 are moderately damaged, and +600 are severely damaged.

Table 2.2. Grattan-Bellew DRI Feature and Factor 1992

<b>Feature</b>	<b>Factor</b>
Coarse aggregate with cracks	0.25
Coarse aggregate with cracks and gel	2
Coarse aggregate debonded	3
Reaction rims around aggregate	0.5
Cement paste with cracks	2
Cement paste with cracks and gel	4
Air voids lined with gel	0.5

Table 2.3. Sanchez DRI Feature and Factor 2014

<b>Feature</b>	<b>Factor</b>
Closed/tight cracks in coarse aggregate particle	0.25
Opened cracks or network of cracks in coarse aggregate particle	2
Opened cracks or network of cracks with reaction product in coarse aggregate particle	2
Coarse aggregate debonded	3
Disaggregated/corroded aggregate particle	2
Cracks in cement paste	3
Cracks with reaction product in cement paste	3

## 2.3 Monitoring

### 2.3.1 Expansion Readings

A common method for monitoring concrete affected by ASR is expansion readings. Gage studs are installed into the concrete in a square, generally 20 in by 20 in. A strain gage is used to measure the length of each side of the square. These readings are taken while the ambient conditions are similar, so that temperature and humidity do not affect the results. The analysis of the expansion of the concrete along with other laboratory tests can aid in deciding what preventative measure is needed for the concrete.

### 2.3.2 Cracking Index

The Cracking Index (CI) is commonly used in conjunction with expansion readings. The CI requires that a 20 in by 20 in (0.5 by 0.5 m) square grid be drawn on the surface of the concrete. The grid is drawn over the most severely cracked section of the concrete. Within the grid, cracks of width 0.05 mm or greater are measured and their widths recorded by what section of each axis they are located on. Map-cracking and cracks bigger than 0.15 mm are reported to indicate a high level of distress in the concrete. Measurements should be taken under similar conditions in order to neglect temperature and humidity effects. The total width of cracks, the average width, and the average crack width per 40 in (1 m) (CI) are calculated. If the cracking index is above 0.5 mm/m, then the concrete is considered to be severely cracked. The change of CI over time can aid in determining a preventive measure for the concrete (Fournier 2010).

### 2.4 Prevention of ASR

There are four different options to prevent ASR in concrete: Limit the alkali content, prevent the use of reactive aggregates, use supplementary cementitious materials (SCMs), and use lithium nitrate.

Limiting the alkali content of cement below 0.6 percent will reduce the amount of alkalis present during mixing. With fewer alkalis, there will be less hydroxyl ions and a lower pore solution pH which will prevent the reactive silica from dissolving to form ASR gel (Stanton 1940). In the United States and Canada the average alkali content of cement is 0.55 percent, though the range is from 0.05 to 1.2 percent (Gebhardt 1994). Based on this data, it is difficult for some regions to obtain cement with less than 0.6 percent alkali content. Additionally, there have been some studies that have shown that achieving an alkali content of less than 0.6 percent

may not eliminate the chance of ASR forming (ACI221 1998). Overall, if the cement has an alkali content of under 0.6 percent, then there is a reduced risk that ASR will occur.

Reactive aggregates, whether fine or coarse, will cause ASR to form in the presence of high alkali cement. To reduce the amount of reactive silica in the concrete mix, it is recommended that nonreactive aggregates be used. However, it is generally not economical to switch aggregates because local aggregates are less expensive to use than farther away aggregates that need to be shipped. To determine if an aggregate is reactive, a mortar bar test can be performed to determine the aggregate's reactivity. Testing though can be costly, and with numerous quarries across the country and varying geologic characters in those quarries make it nearly impossible to determine if an aggregate is reactive. It should be noted that not all aggregates are reactive and if a nonreactive aggregate is available locally, then it should be used to reduce the risk of ASR (ACI221 1998).

Fly ash, silica fume, and slag cement are all SCMs that can be used to reduce the risk of ASR. All of them are used to replace a certain percentage of cement. Reducing the amount of cement will lower the alkali content. Also, SCMs produce a lower C/S ratio, meaning that the CSH that they produce can entrap more alkalis and reduce the pH of the concrete pore solution. Finally, due to their smaller size, they produce a denser paste which lowers the permeability of the concrete (ACI221 1998).

The use of Class F fly ash at a 15 to 30 percent replacement rate will reduce the risk of ASR. Class F is preferred over Class C because it contains fewer alkalis (Thomas 2001a). Silica fume can reduce the risk of ASR when used at 10 to 15 percent replacement (Thomas 2001b). Using a replacement of 25 to 50 percent slag cement can reduce the risk of ASR (ACI221 1998).

All SCMs contain some amount of alkalis. When the amount of alkalis introduced to the concrete mix is less than that of the cement it replaced, and then replacement may be a valid option. Testing SCMs with local reactive aggregates will help determine how much replacement is needed to reduce expansion from ASR below recommended levels.

In 1951, McCoy and Caldwell learned that the use of lithium can prevent ASR. They learned that several different lithium salts stopped ASR from forming (McCoy and Caldwell 1951). When lithium is added to the concrete mix, it reacts with the silica in the aggregates to prevent other alkalis from reacting with the silica. Even though lithium is an alkali, it does not create an expansive gel like other alkalis (Folliard 2006). Some lithium salts such as lithium fluoride and lithium hydroxide have a pessimum effect on ASR. This means that if not enough lithium fluoride or hydroxide is added to the concrete mix, then ASR expansion will increase due to increasing hydroxide amounts. In 1997, Stokes determined that lithium nitrate does not have a pessimum effect. Since the hydroxide concentration does not increase with lithium nitrate, the pH of the pore solution remains closer to seven. The amount of lithium nitrate needed to prevent ASR is determined from the molar ratio of lithium to sodium plus potassium. Lithium nitrate is has a molar ratio of 0.7 (Stokes 1997).

## 2.5 Mitigation of ASR

Based on the extent of damage that the concrete has experienced due to ASR an appropriate treatment can be applied. For damage that is less severe (little to no pop outs or open cracks), topical treatments of linseed oil, silane, or lithium may be used to mitigate ASR. First, linseed oil works as a sealer to keep water out of the concrete and away from the ASR gel. After linseed oil is applied to the surface it dries leaving behind particles that clog the pores on the concrete surface. While water cannot penetrate the surface to enter the concrete, any water that



is within the concrete when the linseed oil is applied cannot escape the concrete. Water that is trapped inside the concrete will allow ASR to continue to expand (Wright 1993).

Second, silane is another sealer that when applied bonds to the concrete surface to form a hydrophobic layer. This seal prevents water from entering the concrete, which stops ASR from further expanding. Silane not only prevents water from entering the concrete, but allows moisture already in the concrete to escape. The moisture loss from the concrete should keep the relative humidity in the concrete below 80% (Lute 2008).

Third, lithium nitrate can be used to mitigate ASR. The liquid lithium nitrate penetrates the concrete surface and reacts with the silica to stop more ASR gel from forming (Folliard 2006). However, spraying lithium nitrate onto the concrete surface does not allow it to penetrate more than 50 mm (Stokes 2002). Such a shallow penetration does not stop ASR gel from forming in deeper sections of concrete. Also, moisture is not prevented from entering the concrete, so already existing ASR gel will continue to expand. Another disadvantage to lithium nitrate is that it is expensive.

Fourth, to counter the limited depth of penetration, vacuum and electrochemical impregnations of lithium have been developed. Electrochemical impregnation works by placing a saturated mat of lithium on top of the concrete and then establishing an electrical circuit with the reinforcing steel, mat, and voltage source. The reinforcing steel acts as the negative charge while the mat maintains a positive charge. Since lithium has a positive charge it is attracted to the reinforcing steel and drawn into the concrete. This method allows lithium to reach greater depths in the concrete (Thomas 2007). However, lithium rarely reaches deeper than the reinforcing steel. Given the use of the concrete (column, slab, etc.) this either has no impact or has a large impact on ASR expansion. In a column, the reinforcing generally forms a cage which

prevents expansion. Therefore, electrochemical impregnation on a column would stop ASR expansion because it stops ASR outside the reinforcing steel, while the steel cage prevents expansion. In a concrete slab, the reinforcing steel usually runs one direction and does little to stop ASR expansion. While lithium may be able to penetrate down to the reinforcing steel, the concrete below the steel can still experience ASR formation. Since most reinforcing steel in a concrete slab is placed with minimum cover, ASR expansion can cause cracking in the bottom of the slab. The cracks that form will allow water to enter the concrete and start affecting the steel. Again, lithium in the concrete does not stop moisture from entering, so any ASR gel that is present will continue to expand. The treatment time for electrochemical impregnation is 4 to 8 weeks, which is much longer than a day long lane closure for spraying lithium nitrate. Just like lithium nitrate, electrochemical impregnation is expensive (Thomas 2007).

Fifth, vacuum impregnation is another method used to get lithium to penetrate deeper into the concrete. In vacuum impregnation, a sealed “box” is created over a certain area of concrete that is to be treated. Then, a vacuum is created in the box down to 0.5 atm. Lithium is then sprayed into the box and absorbed into the concrete (Thomas 2007). This mitigation technique is expensive.

The final mitigation technique is to confine the concrete. This technique does not work well with pavements, but rather with barrier walls and columns. The concrete that is affected by ASR is wrapped with a carbon fiber fabric held together with high strength epoxy. The wrap will resist any expansion due to ASR. Another benefit of the wrap is that it will keep water out of the concrete. However, the wrap is expensive (Thomas 2013).

## 2.6 Freeze-Thaw

Freeze-thaw damage appears in concrete after pressures from water freezing exceed the tensile strength of the concrete. As water freezes in the concrete pore structure, unfrozen water tries to reach equilibrium by moving from unfrozen pores towards frozen pores. Osmotic pressure builds up due to the resistance of the unfrozen water to flow while trying to create an equilibrium concentration (Powers 1975). When this pressure grows larger than the concrete's tensile strength cracking occurs.

According to T. C. Powers in 1945, ice exerts 736psi per °F below the freezing point. For example, if the temperature is 15°F, then the pressure that ice exerts is 736psi times the change in temperature, 17°F. This principle only applies between 32°F and -4°F, at which the pressure that ice exerts reaches its maximum of 29,000psi. Powers uses this information to determine at what temperature concrete will crack due to ice formation. Concrete's resistance to cracking is called its tensile strength. A general rule of thumb is that concrete's tensile strength is approximately 10% of its compressive strength. There are two assumptions made by Powers. First, that 10% of mobile water is in contact within the cross-section. Second, that the stresses adjacent to the source of pressure are higher and therefore only half the stress is present elsewhere. Given these assumptions and information, a formula can be developed to determine the temperature at which concrete will crack (Powers 1945).

$$^{\circ}\text{F} = 32^{\circ}\text{F} - 0.000679f'c$$

When cement hydrates it grows to more than twice its size. This occurs because the cement is using up water, so the volume of water needs to be taken up by the volume of the hydrated cement. The structure of hydrated cement is random and leaves small pores that water cannot freeze in. Water that is within the cement structure once hydration is reaching its end stages is used, evaporated, or trapped. This leaves small interconnected channels in the cement

gel (dried). These spaces are capillary pores. They are large enough for water to freeze in them (Powers 1955). They are generally 1 to 10mm in size (Henderson 2006).

Sodium and Potassium Hydroxide are common in hardened paste. They will dissolve into water that is in the concrete. The alkali solution will have a lower freezing point than that of “pure” water (Powers 1955).

Larger pores generally freeze at a higher temperature than smaller pores. The temperature difference created by pore size is larger than the temperature difference created by alkalis (Powers 1975).

Freeze thaw was originally believed to be caused by the 9% expansion water experiences when it freezes. That expansion along with the concrete being 91.7% full of water during freezing would cause the concrete to crack. However, this theory assumes that concrete is a closed vessel, which is not the case. Concrete has many pores on the surface. As ice forms, unfrozen water can be pushed to the surface or an unfilled pore (Powers 1975).

Power proposed in 1945 that cracking due to freeze thaw was caused by hydraulic pressure. By treating concrete as an open vessel that allowed water to flow through capillaries to other pores as water froze in a pore. The water that is flowing through the capillaries creates pressure in the concrete (Jansen 1994).

While Hydraulic Pressure Theory worked to explain cracking in concrete during freeze thaw, it does not address why concrete expands even when temperature is constant. Powers and Helmuth in 1953 proposed that osmotic pressure also contributed to pressures inside the concrete that caused cracking (Powers and Helmuth 1953). Since there are different temperatures occurring in the concrete during freezing, the water is trying to reach thermodynamic equilibrium. To reach equilibrium, water travels toward a pore that has ice. This happens since

when ice forms the “pure” water freezes first and then the water with alkalis. To counter the high concentration of alkalis that are unfrozen, water from the surrounding area moves towards that pore to achieve equilibrium. However since the opening to pores and capillaries are small, the diffusion into the pore creates an osmotic pressure. The amount of pressure caused by osmosis is dependent on the concentration of alkalis (Powers 1975).

Freeze thaw can also be caused by aggregates in the concrete. Aggregates generally have larger pores than the cement paste. These larger pores allow water to freeze just below the normal freezing point. Most cracking and pop-outs are caused by hydraulic pressure, though some aggregates have small pore structures like cement paste (Powers 1975). D-cracking starts with aggregates that are susceptible to freeze thaw. The resulting freeze thaw cracks run parallel to the slab joint and curve out into the slab near the corners. These cracks make the concrete look darker and appear to be in a D shape with the curve of the D along the joint edge and the corners. D-cracking takes five to ten years to form and the depth of freezing also affects the rate of D-cracking (Jansen 1994). Scaling can also occur on the surface of concrete due to freeze thaw. This is due to a weak surface layer that allows moisture in and peels up due to freeze thaw (Walker 2006).

## 2.7 Test Methods for Determining Freeze-Thaw

There are two ways to determine if freeze-thaw is the cause of deterioration in concrete. The first way is through testing an aggregate’s susceptibility to freeze-thaw. The second way is by visual inspection.

### 2.7.1 Aggregate Susceptibility

#### 2.7.1.1 AASHTO T 104/ASTM C 88 (Sulfate Soundness)

Sulfate Soundness is described in AASHTO T 104 and ASTM C 88. The purpose of sulfate soundness is to determine if a fine aggregate is susceptible to freeze-thaw. Preparation of either sodium sulfate or magnesium sulfate and fine aggregate gradation is included in the AASHTO T 104 and ASTM C 88. The aggregate is submerged in solution for 16 to 18 hr at 70°F. After the immersion period, the solution is drained off the aggregate. The aggregate is placed in the oven at 230°F until a constant weight is achieved. The submersion and drying is repeated till the number of cycles chosen is complete. After the final cycle, the aggregate is washed with barium chloride solution at 110°F and then dried again. The aggregate is then sieved by hand and the weight retained on each sieve is recorded. The percentage loss of each fraction is recorded. A fine aggregate is considered susceptible if the average weighted loss is greater than 10% with sodium sulfate or 15% with magnesium sulfate after 5 cycles.

#### 2.7.1.2 AASHTO T 161/ASTM C 666 (Rapid Freezing and Thawing)

Rapid Freezing and Thawing is described in AASHTO T 161 and ASTM C 666. The rapid freezing and thawing test is used to determine if an aggregate is susceptible to freeze-thaw. The freeze-thaw chamber, scales, comparator, and dynamic testing apparatus are defined in the specifications given above. Regardless of the procedure chosen, the testing procedure is the same. Concrete specimens are cured for 14 days before testing, or if the specimens were cored, they are saturated with lime water for 48 hrs. Then the specimens are placed in the freeze-thaw chamber. The specimens are exposed to a chosen number of freeze-thaw cycles. Each freeze-thaw cycle is a temperature change of 40°F to 0°F to 40°F. The freeze-thaw cycle should be at least 2 hrs. in length, but no more than 5 hrs. Each specimen is to be measured no more than 36 cycles apart. Each measurement includes determining the dynamic modulus of elasticity, mass

loss, and length change. Three hundred cycles, 60% of the original dynamic modulus of elasticity, or 0.1% length change can be chosen as the end of testing.

At the end of testing, the mass loss, expansion, and dynamic modulus of elasticity loss are recorded. The Durability Factor (DF) is calculated using the dynamic modulus of elasticity. The DF is used to determine if an aggregate is susceptible to freeze-thaw.

## 2.7.2 Visual Inspection

### 2.7.2.1 Petrography

Visual inspection of concrete structures affected by freeze-thaw is generally done by petrographers. The inspection is mainly done in a laboratory, but a visual inspection of the concrete in the field should also be done to identify scaling, pop-outs, and D-cracking. Once cores have been removed from the concrete structure, then petrographers look for laminations in the concrete that would indicate freeze-thaw. The core are examined under a microscope for an adequate air void system. Cracking around and through aggregates is recorded along with cracking through the cement matrix (Walker 2006).

## 2.8 Prevention of Freeze-Thaw

Aggregates have a larger pore structure than cement paste. The water in the pores can freeze at temperatures near the normal freezing point. When freezing occurs, the aggregates freeze cracking the concrete or causing a pop out. This can be controlled using aggregates that have a smaller pore structure and permeability (Powers 1955). Reducing the maximum aggregate size also reduces the chance of cracking (Jansen 1994).

Proper finishing can reduce the risk of freeze thaw damage in concrete. The top of the concrete generally has a higher paste fraction than the rest of the concrete. Bleeding,

compaction, finishing, and curing conditions determine how much paste is at the surface of the concrete. Bleeding can be reduced by adding less water to the mix. Concrete should be compacted properly into the forms to ensure that there are no large air voids. This can be achieved using vibrators or rodding. However with air entrained concrete over vibration must be avoided because it could pop the air bubbles reducing the impact of air entrainment. Finishing the concrete surface not only creates a smooth surface, but reduces surface area and voids for water to penetrate into the concrete. Proper curing methods, such as wet burlap or misting are necessary for the concrete to gain strength and to decrease its permeability.

Air entrainment works to reduce the distance water must travel in the capillaries. This decrease in travel length allows the pressure generated by moving water not to exceed the tensile strength of the concrete. The optimal spacing factor for air entrainment is 0.006in. Also, air entrainment is much smaller (0.01 to 1mm) than normal voids, entrapped air voids (1 to 10mm) (Henderson 2006). Water that is in these smaller voids will freeze at a lower temperature; therefore, making the concrete more freeze-thaw resistant. One to two percent air is naturally entrapped in concrete, and a rule of thumb to have adequate freeze thaw resistance is to have a total air content (entrapped plus entrained air) of  $6 \pm 1$  percent air in the concrete (Henderson 2006).

## 2.9 Mitigation of Freeze-Thaw

Once freeze-thaw has been determined as the cause of deterioration, there are several options to stop further freeze thaw. Overlaying the existing concrete with asphalt can be used to reduce the amount of moisture entering the concrete and to reduce the depth of frost in the concrete. Reducing the amount of moisture and increasing the depth prevents there from being sufficient moisture for freezing to occur.



The use of Linseed oil to prevent freeze thaw has been used since the 1960s. Linseed oil works as a sealer to prevent moisture from entering the concrete. It is applied as a liquid onto the concrete surface and is left to dry. The linseed oil will penetrate into the concrete and then dry. The linseed oil particles that are left after drying clog the pores of the concrete preventing moisture from entering the concrete. Linseed oil penetrates deeper than most other sealants and therefore is not as affected by abrasion. However, moisture in the concrete cannot escape easily once linseed oil is applied. This trapping of moisture can worsen the effects of freeze thaw (Wright 1993).

Silanes are becoming more popular than linseed oil because they allow moisture to escape the concrete. Silanes are another type of sealer that bond with the concrete surface rather than clogging pores. The seal is hydrophobic so that water is repelled away from the concrete. Silane does not penetrate as deep as linseed oil because it bonds with the surface. Since the surface is the only area that silane bonds with is the surface, silane is affected by abrasion (Wright 1993).

Grinding down the top surface can help prevent freeze thaw. If the top layer is weak or highly permeable, then removing that layer can allow a less permeable and stronger layer to be at the surface. Grinding can also be used to affect how water runs off the concrete. Removing water from the concrete will prevent the concrete from reaching sufficient saturation for freeze thaw.

The last option is to replace the concrete. When the concrete cannot be sealed due to large potholes and the surface cannot be grounded, then replacement may be the best option. An asphalt overlay may not work if the concrete is damaged to the point that it is not a suitable base

layer. Before any remediation is done, there should be an evaluation to determine the best method to remediate the concrete.

## 2.10 Purpose of Research

Even though there has been ASR research conducted in other states, Arkansas has only recently started looking into ASR because of premature pavement and barrier wall deterioration on I-49. Since I-49, a couple of other interstates, I-30 and I-530, in central Arkansas and the runway at Northwest Arkansas Regional Airport have started to show premature deterioration. Research on these pavements and the potential reactivity of aggregates across Arkansas has started at the University of Arkansas (UA) (Deschenes 2014). ASR has been found to be the cause of the deterioration and a couple aggregates have been determined to be slightly reactive (Deschenes 2014). Part of this research is to discover how much damage has taken place within concrete pavements throughout Arkansas using DRI. The next part of the research is to perform the PFET on cores taken from I-49 to determine how much expansion has yet to occur in the pavement.

While research on sealers for mitigating ASR has mainly occurred at the University of Texas at Austin (UT) and Laval University (LU), no research on sealers in Arkansas has been conducted which is a mixture of their climates (Lute 2008 and Berube 2002). Arkansas has hot and humid summers, like UT, and cold winters, like LU, which allow ASR and freeze-thaw to occur respectively. The I-49 pavement not only has shown map-cracking (ASR), but D-cracking (freeze-thaw). The final part of this research is to look at the use of sealers to mitigate ASR and freeze-thaw in concrete pavement blocks.

### **3 Methods and Materials**

#### **3.1 Experimental Program**

The first part of this research is to determine the extent of damage in I-49, I-30, and I-530 concrete pavements in Arkansas. The Damage Rating Index will be used on cores from each pavement to quantify the damage. The presence of ASR gel and other notable features will be presented to confirm or contradict that ASR is the main cause of distress.

The second part of this research is to determine how much more expansion is likely to occur in the I-49 pavement. The Potential for Further Expansion test will be used. The amount of expansion will be documented along with how the expansion will affect the pavement.

The third part of this research is to determine a sealer that will mitigate ASR and freeze-thaw expansion in concrete pavements. Concrete blocks induced with ASR, exposed to freeze-thaw, and sprayed with different sealers will be used. The expansion will be monitored and reported. The sealer that reduces expansion the most will be considered to have mitigated ASR and freeze-thaw the best.

#### **3.2 Damage Rating Index**

As explained before the Damage Rating Index (DRI) was created to give a semi-qualitative measurement of the extent of damage within hardened concrete. Several coring operations on interstate pavements have taken place across Arkansas (locations are discussed in Chapter 3 Section 1), so that petrographic examination and DRI can determine the current state of the several interstate pavements. The DRI analysis, which was performed at the UA, was conducted in accordance to the procedure developed by Grattan-Bellew in 1992 (Gratten-Bellew 1992). An overview of the test method is described below.

After the 4 inch diameter cores (approximately 12 inches in length) were removed from the pavement, they were sealed in bags or boxes and shipped to the UA. Once they arrived to the UA, the cores were removed from their bags or boxes and were examined for any rebar, cracks from coring, or other abnormalities. After examination, the cores were cut into two halves, lengthwise with a concrete saw. The saw was a wet saw, though the presence of water was reduced to avoid washing away any ASR gel deposits. Care was also taken while sawing to keep a straight line and avoid deep saw blade marks into the cores.

One of the halves was then polished. The polisher was a Gison GPW-211. It was powered by an air compressor and the head was capable of dispensing water while polishing. The amount of water that was dispensed could be controlled, so that ASR gel deposits would not be washed away. The head was 4 in diameter and Velcro capable. Diamond polishing pads with a 4in diameter were used for polishing. The grits used were 50, 100, 200, 400, 800, 1500, and 3000. Table 3.1 provides the amount of time each grit was used to ensure the core was smooth and without scratches. Halfway through each grit the core was rotated 180°

Table 3.1. Grit Times

Grit	Time (min.)
50	20
100	10
200	5
400	5
800	5
1500	5
3000	5

During polishing, two patterns were employed to avoid creating grooves in the surface of the core. Figure 3.1 shows the two patterns used, in which the green dot represents the start, the yellow dot represents turning around, and the red dot represents the stopping place. Each pattern was performed three to four times before switching to the other pattern. Patterns were also

started from the right side of the core just in case starting from one side created grooves or affected the smoothness. Overlapping passes in each pattern helped to reduce grooving and improve smoothness.

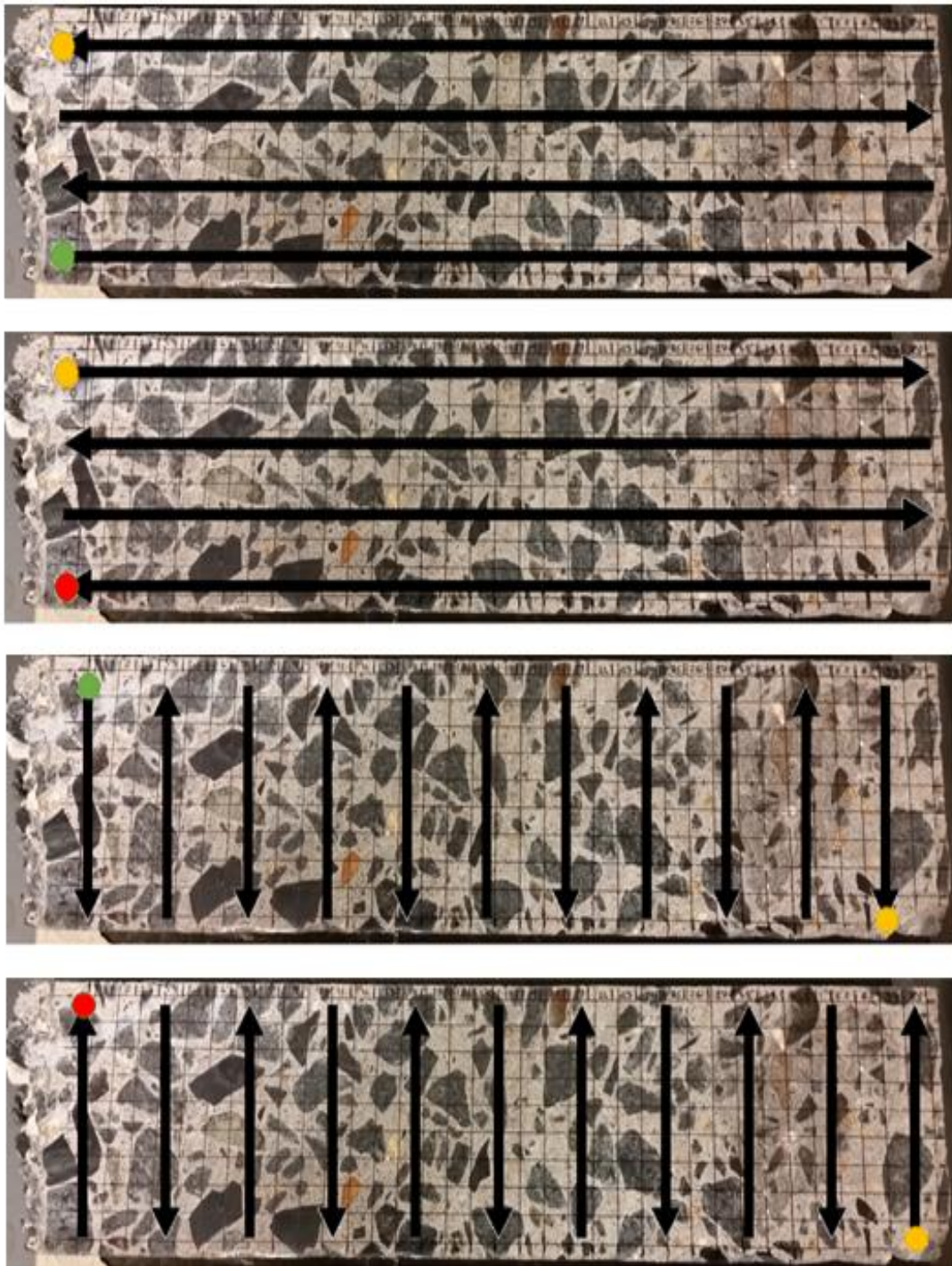


Figure 3.1. Polishing Patterns

The speed of which the polisher was moved across the surface of the core was kept to one to two seconds down the length of the core. This speed reduced the time for polishing and the

roughness of the core. Starting and stopping, falling off the core, and staying still were all kept to minimum to prevent the formation of deep scratches or grooves.

After polishing, the cores were allowed to dry at room temperature. They were then visually inspected for any remaining scratches that needed to be removed by further polishing. If no scratches were found, then the cores were marked with a 1cm by 1cm grid. At least 0.5cm was given between the edge of the core and the edge of the grid. This distance was provided to make sure that any cracks from coring or sawing that existed on the outside of the core did not get included in the DRI count. If more than 0.5cm was needed due to asphalt intrusion, then extra space was given and the grid made smaller.

A microscope was used to count the individual features in each 1cm by 1cm square. The microscope used was an Amscope Simul-Focal Boom Stereo Microscope. It has the ability to achieve the 15x or 16x magnification required for DRI. The microscope also has a camera to take pictures of features on cores.

As each individual feature was counted per 1cm by 1cm square, it was input into an excel spreadsheet that applied the appropriate factors to each feature. If no specific feature existed in a square, then no factor was applied for that feature for that square. The sum of each feature was multiplied by its factor and then divided by the total area examined. At least  $200\text{cm}^2$  of the surface area of each core was examined. Each feature was then multiplied by  $100\text{cm}^2$  to normalize the core, so that it could be compared with other cores. The normalized feature was then summed with the other features to obtain the Damage Rating Index Number. The features are explained in Table 3.2.

Table 3.2. Petrographic features & weighing factors (Villeneuve 2012).

<b>Petrographic features</b>	<b>Factors</b>	<b>Comments</b>
Closed/tight cracks in coarse aggregate particle	0.25	<ul style="list-style-type: none"> <li>• Tight/fine cracks showing no gap at 16X magnification;</li> <li>• Sometimes “appear” to contain whitish secondary products, as the crack forms an angle with the cutting plane</li> <li>• A low factor is given as such cracks are likely produced by aggregate processing operations (quarried aggregate) or weathering (gravel).</li> </ul>
Opened cracks or network cracks in coarse aggregate particle	2	<ul style="list-style-type: none"> <li>• Crack showing a gap at 16X magnification.</li> <li>• A “network” of cracks is also classified in this category as it is likely caused by expansive reactions within the aggregate particles.</li> </ul>
Cracks or network cracks with reaction product in coarse aggregate particle	2	<ul style="list-style-type: none"> <li>• Cracks containing secondary reaction products (whitish, glassy or chalky in texture)</li> <li>• Sometimes, the secondary products do not fill all the cracks (material lost during the preparation of the polished section)</li> </ul>
Coarse aggregate debonded	3	<ul style="list-style-type: none"> <li>• Crack showing a significant gap in the interfacial zone between the aggregate particle and the cement paste</li> <li>• Would likely cause debonding of the particle when fracturing the concrete.</li> </ul>
Disaggregated / corroded aggregate particle	2	<ul style="list-style-type: none"> <li>• Aggregate particle that shows signs of disintegration, “corrosion” or disaggregation (ex: reacting opaline shale and chert/flint particles).</li> </ul>
Cracks in cement paste	3	<ul style="list-style-type: none"> <li>• Crack visible at 16X magnification, but with no evidence of reaction products.</li> </ul>
Cracks with reaction product in cement paste	3	<ul style="list-style-type: none"> <li>• Cracks containing secondary reaction products (whitish, glassy or chalky in texture)</li> <li>• Sometimes, the secondary products do not fill all the cracks (material lost during the preparation of the polished section).</li> </ul>

### 3.3 Potential for Further Expansion Test

Nine of the cores taken from the I-49 pavement in the summer of 2014, were used for the Potential for Further Expansion Test developed by Stark in 1991. The drilled cores were 4 in. diameter and 13 in long depending on asphalt subgrade thickness. The layer of asphalt was sawn off, so that each core was an equal length of 10 in. A drill was used to bore holes into the center



of each end of a core for gage studs. The gage studs were fitted into the holes, leaving a quarter inch outside the concrete, and epoxied into place. Each core was then labeled with its mile marker and given a number to differentiate them throughout the test.

Normally, three-five gallon buckets would be used to store the nine cores in a water bath, but due to a lack of Styrofoam, three-6 in by 12 in cylinder molds were used for the 1N NaOH solution cores. The first-five gallon bucket was fitted with two wooden blocks with 1 in height at the bottom, so that 1 in. of water at the bottom could be easily measured and maintained. Above the wooden blocks, a piece of Styrofoam was cut to fit into the bucket and rest on top of the wooden blocks. Three small holes were cut just big enough in the Styrofoam for the gage studs to fit in. The cores would rest on the Styrofoam, while the gage studs would not carry any of the weight of the cores being in the holes. Four inches from the top of the bucket another Styrofoam piece was place with three holes cut into it symmetrically about the center. These holes were made just bigger than four inches to accommodate the cores. The sides of the bucket were lined with a towel. The towel was taped to the top of the bucket, while the bottom of the towel sat above the bottom piece of Styrofoam. Figure 3.2 shows the cores in the first bucket. A lid fitting over the bucket and towel was used to create a watertight seal.



Figure 3.2. Bucket with Cores over Water

The second-five gallon bucket was fitted with a piece of Styrofoam at the bottom of the bucket. Like the first-five gallon bucket, small holes were cut into it for the gage studs. Four inches from the top of the bucket a piece of Styrofoam was placed with three holes cut into it symmetrically about the center. The holes were cut a little bigger than four inches to accommodate the cores.

Three 6 in. by 12 in. cylinder molds were fitted with a piece of Styrofoam at the bottom of the mold. Each piece of Styrofoam had one small hole cut into it for a gage stud. No Styrofoam was used in the top because the cores could sit inside the molds without touching the sides. Each cylinder had a lid for a water tight seal.

Each bucket or cylinder was then filled with its appropriate liquid. The first bucket was filled with 1 in of water at the bottom. The second bucket was filled with tap water at 73°F to just 1 in under the top of the bucket. All three cores were in the bucket during filling to ensure that it did not overflow and that the cores were completely submerged. The three cylinders were filled with 1N NaOH solution till each core was completely submerged.

A water bath was prepared using a 100 gal watering trough. The water temperature was measured and controlled using an electric thermometer connected to a heater. The water bath was maintained at 100°F. All the buckets and cylinder molds were kept in the water bath throughout the testing. The buckets were not submerged in the water bath, but the water came up to just under the lid for the buckets, which is shown in Figure 3.3. The two extra buckets in Figure 3 were for another project not discussed in this paper.



Figure 3.3. Water Bath

The initial length for each core was recorded using a length change comparator which is shown in Figure 3.4. The cores were then placed into their respective buckets and placed into the water bath. Subsequent readings were taken every week for one year. Before each reading, the buckets were removed from the water bath and placed into an environmental chamber at 73°F. The buckets were allowed to cool for at least 16 hr. Each core was then removed from the buckets and measured twice using the length change comparator. The cores were measured the same way every time to ensure equivalent readings. After the lengths had been recorded, the cores were placed back in the bucket but the cylinders were flipped, so that one end of the core did not always take the weight of the core. The buckets were then returned to the water bath. At six months, the 1N NaOH solution in the cylinders was replaced.



Figure 3.4. Length Change Comparator

The strain for each set of cores was calculated in excel by doing the following. First, the weekly two readings of a core were averaged together. Second, the initial reading for that core was subtracted from the average reading of that week to obtain the displacement. Third, the displacement was divided by the original length of the cores and multiplied by 100% to obtain the strain as a percent. Fourth, the percent strain for each core in a set was averaged together to get the percent strain of the set.

#### 3.4 ASR and Freeze-Thaw Mitigation by Sealers

The I-49 pavement is currently experiencing distress due to ASR and freeze-thaw. With both ASR and freeze-thaw deteriorating the concrete pavement, it was determined that any mitigation technique would have to counteract both causes of distress. Before any application of treatment to the pavement it was decided to test in the lab which mitigation technic would work

the best to limit ASR and freeze-thaw. Two mitigation techniques were found to reduce ASR and freeze-thaw, linseed oil and silane. Also given the project's close relation with AHTD, they requested that topical lithium be tested.

Originally nine concrete exposure blocks were cast at the UA. The mix design for seven of the nine blocks is given in Table 3.3, while the mix design for the remaining two blocks is explained below. Seven of the blocks were made with a Type I high alkali cement (0.9% alkalis). The coarse aggregate was a local limestone that is known to not be reactive. The fine aggregate was a combination of local slightly reactive Arkansas River sand and reactive Jobe sand from El Paso, Texas. The Jobe sand was used at a 20% replacement rate. Additional alkalis were used in the form of NaOH pellets to accelerate ASR. The other two blocks had the same mix design, but received no Jobe sand or additional alkalis by mistake. However, the blocks were kept to see the result of Arkansas River sand reacting with the high alkali cement. No air entrainment was used. These blocks will be referred to as Group 1, and they were cast in November 2014.

Table 3.3. Mix Design Group 1

Material	Quantity (lb/yd <sup>3</sup> )
Cement	611
Coarse Aggregate	1710
Fine Aggregate (River Sand)	1183
Fine Aggregate (Jobe Sand)	296
Water	236
NaOH	2.86

To assess each treatment's ability to mitigate ASR and freeze-thaw, another fourteen concrete blocks were made. These blocks were cast using the mix shown in Table 3.4. Type I

cement with an alkali content of 0.9% was used in conjunction with a combination of highly reactive Jobe sand from El Paso, Texas and local slightly reactive Arkansas River sand to produce ASR. While Arkansas River sand is known to be slightly reactive, the reaction does not happen quickly enough for laboratory testing. To accelerate the test, Jobe sand was used at a replacement rate of 30% for the total fine aggregate. The coarse aggregate was a non-reactive limestone from a local quarry. The water to cement ratio was 0.44. Additional alkalis were introduced into the mixing water by NaOH pellets to ensure ASR would occur. No air entrainment was used. These blocks will be referred to as Group 2, and they were cast in July 2015.

Table 3.4. Mix Design Group 2

Material	Quantity (lb/yd <sup>3</sup> )
Cement	611
Coarse Aggregate	1710
Fine Aggregate (River Sand)	1035
Fine Aggregate (Jobe Sand)	444
Water	236
NaOH	2.86

The concrete was mixed and placed into two forms that were two feet by two feet by eight inches deep as shown in Figure 3.5. The bottom of the forms was made of plywood with four holes, so that gage studs could be placed into the concrete. As the concrete was placed into the forms, it was rodded and consolidated. After the concrete was placed, the surface was finished with a trowel.



Figure 3.5. Formwork

The blocks were removed from the forms one day after casting and placed outside on a bed of gravel. The side with the gage studs faced up. The blocks were cast within 14 days of each other to provide accurate expansion data. The blocks were allowed to cure 1 month before the initial expansion reading was taken using a Demec gage. Following the initial reading, the blocks were then treated.

The Group 1 blocks were treated with a linseed oil and a silane. The treatments are given in Table 3.5. Two blocks were used as controls. The silane was Enviroseal 40 (now MasterProtect 400 H) by BASF and applied to three of the blocks (BASF). The linseed oil was from Euclid Chemical and was applied to the remaining for blocks, which includes the two blocks without Jobe (Euclid Chemical). The manufacturer's application rate was used for all treatments. Group 1 was treated at one month.

Table 3.5. Treatments Group 1

Treatment	1 Month	Application Rate (square foot per gallon)
Control	X	-
Enviroseal 40 (Silane)	X	150
Euclid (Linseed Oil)	X	300

Table 3.6 gives the different treatments that were applied to the Group 2 blocks. Each treatment was applied to two blocks. The three silanes that were examined were Enviroseal 40 by BASF, Sikagard 740W by Sika, and Barricade 100 by Euclid Chemical (BASF, Sika, and Euclid Chemical). The linseed oil used was produced by Euclid Chemical (Euclid Chemical). The lithium was Lithium-825 and provided by Sinak Corporation (Sinak Corporation). The manufacturer’s application was used for all treatments. Group 2 was treated at one month with a pair of lithium blocks treated again at 1 year. The chemical composition of each treatment is given in Table 3.7.

Table 3.6. Treatments Group 2

Treatment	1 Month	1 Year	Application Rate (square foot per gallon)
Control	X	-	-
Enviroseal 40 (Silane)	X	-	150
Sikagard 740W (Silane)	X	-	150
Barricade 100 (Silane)	X	-	200
Euclid (Linseed Oil)	X	-	300
LS-825 (Lithium)	X	-	150
LS-825 (Lithium)	X	X	150



Table 3.7. Chemical Compositions of Treatments

Treatment	Composition
Enviroseal 40	40% Silane Water Based
Sikagard 740W	40% Silane Water Based
Barricade 100	100% Silane
Linseed Oil	50% Solids by Volume 40-70% Linseed Oil 40-70% Mineral Spirits
Lithium-825	6% Lithium 36% Sodium Silicate 58% Water

The blocks were measured at least once every month to determine the amount of expansion each treatment due to ASR and freeze-thaw. Measurements were taken when the blocks were dry and as close to 70°F air temperature as possible. To determine if freeze-thaw had taken place in the concrete, relative humidity probes that could measure temperature to the nearest 0.02°F were used (LabJack Corporation). The humidity probes were installed in the first control block in the Group 2 blocks. They were placed 1.5 in and 3 in into the concrete to determine the depth of frost. The probes were installed in late November and removed in late February when temperatures are coldest in Northwest Arkansas. Precipitation data was obtained from the National Oceanic and Atmospheric Administration (NOAA). The precipitation data combined with the temperature data was used to determine if freeze-thaw cycles occurred.

## **4 Results and Discussion**

### **4.1 Experimental Program**

The first part of this research is to determine the extent of damage in I-49, I-30, and I-530 concrete pavements in Arkansas. The Damage Rating Index will be used on cores from each pavement to quantify the damage. The presence of ASR gel and other notable features will be presented to confirm or contradict that ASR is the main cause of distress.

The second part of this research is to determine how much more expansion is likely to occur in the I-49 pavement. The Potential for Further Expansion test will be used. The amount of expansion will be documented along with how the expansion will affect the pavement.

The third part of this research is to determine a sealer that will mitigate ASR and freeze-thaw expansion in concrete pavements. Concrete blocks induced with ASR, exposed to freeze-thaw, and sprayed with different sealers will be used. The expansion will be monitored and reported. The sealer that reduces expansion the most will be considered to have mitigated ASR and freeze-thaw the best.

### **4.2 Damage Rating Index**

The cores examined using the DRI were taken from I-530 between exits 30 and 32 near Pine Bluff, Arkansas, I-30 between exits 135 and 138 near Little Rock, Arkansas, and I-49 at mile marker 46 near Winslow, Arkansas. Each pavement was examined to assess the extent of damage. Then comparisons were made between cores taken from the middle of a pavement slab and those cores taken near the joints. Finally, the cores taken from I-49 were examined for evidence of freeze-thaw damage because the I-49 pavement has been showing signs of D-cracking. DRI from each pavement section is discussed in greater detail in the following

sections. Each core was named after the name given to it by AHTD and their abbreviations are given in Table 4.1.

Table 4.1 Labeling Convention

Abbreviation	Meaning
NB	North bound side of interstate
SB	South Bound side of interstate
Mid	Removed from the middle of the slab
Joint	Removed next to the joint between slabs
Corner	Removed from the corner of the slab
SW	Removed from the southwest corner of the slab
M 46	Mile maker 46
M3, C19, BB0202 14-005	Extra markings that do not determine location

#### 4.2.1 I-530 Pavement:

During the spring of 2014, cores were taken from the I-530 pavement near Pine Bluff, Arkansas. The pavement had prematurely been showing signs of map cracking, D-cracking, and spalling. Another two cores were taken from I-530 in early 2015. The DRI for the I-530 cores is given in Figure 4.1. The total DRI for all the cores are given and for each core, the type of distress is shown. Shown below in Table 4.2 are the abbreviations for the corresponding distress which is shown in DRI figures.

Table 4.2 DRI Feature Abbreviations

Feature	Abbreviation
Closed/tight cracks in coarse aggregate particle	CCA
Opened cracks or network of cracks in coarse aggregate particle	OCA
Opened cracks or network of cracks with reaction product in coarse aggregate particle	OCAG
Coarse aggregate debonded	CAD
Disaggregated/corroded aggregate particle	DAP
Cracks in cement paste	CCP
Cracks with reaction product in cement paste	CCPG

As shown in Figure 4.1, the majority of the cores had DRIs that ranged from 200-500. This would signify that the pavement has slight to moderate damage. However, both sides of BB0202 and the single side of SB Mid Slab have high damage with DRIs from 1000-2300. BB0202 was one of the two cores removed in 2015. Therefore it was subjected to additional weathering. However, C19 and BB0202 were cored on the same day, but C19 had a DRI matching that of cores taken in 2014. Since the researcher was not there to watch the coring procedure, BB0202 was most likely removed from a heavily damaged slab.

SB Mid Slab was cored in the spring of 2014. The high DRI number corresponding to SB Mid Slab could be similar to BB0202 in that it was taken from an already heavily damaged slab. However, the DRI number is much lower than that of BB0202, though still high compared to the rest of the cores. Also, the amount of disaggregated particles is less than that of BB0202, while the number of open cracks in the aggregates is higher than the other cores.

The feature count of each core is given in Figure 4.2. The feature count is the summation of each DRI feature. The features are not multiplied by their corresponding factor. This count shows how much of each feature was present, giving a clearer understanding of what damage is in the concrete. For example, two cores could have the same DRI number of 133, but one core could have 1000 CCA, while the other could have 84 CCP. The DRI is the same for both, but the cause of damage is different.

Cores BB0202, C19, and SB Mid Slab were removed by AHTD and their location within the pavement is not known. Therefore, they will not be considered in the overall discussion. The rest of the cores mainly consisted of closed cracks in the aggregate (CCA). There are open cracks in the aggregate (OCA) and cracks in the cement paste (CCP) which contribute about a quarter to a half of the DRI. It was observed that most of the cracks in the cement paste were

located near the surface of the pavement on the core. ASR gel was noticed in all the cores, but not in large quantities as indicated by low OCAG and CCPG counts.

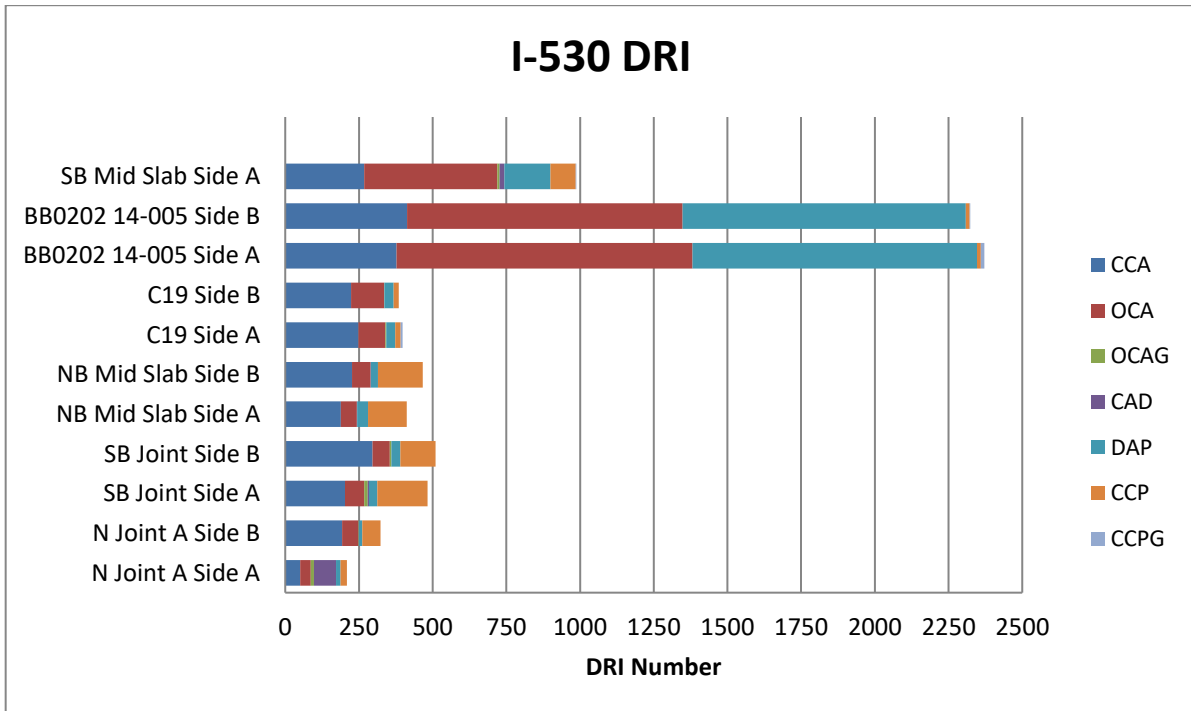


Figure 4.1. I-530 DRI

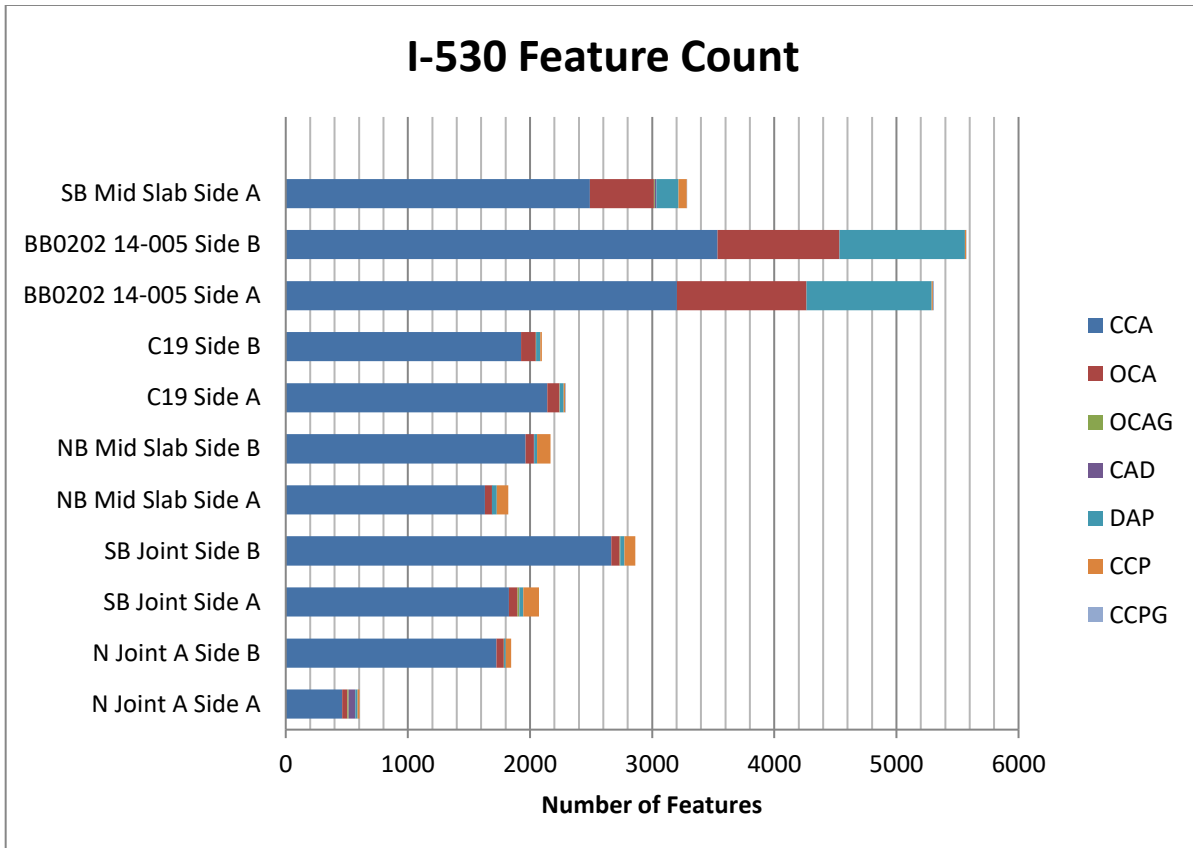


Figure 4.2. I-530 Feature Count

#### 4.2.2 I-30 Pavement:

The I-30 cores were taken near Little Rock, Arkansas in the spring of 2014. I-30 has been showing signs of spalling, map cracking, and D-cracking before its expected life span. The DRI numbers and feature counts for I-30 are shown in Figure 4.3 and Figure 4.4, respectively. The DRI numbers ranged from 1500-2500, which signifies severe damage of the concrete pavement. The majority of the cracking was due to closed cracks in the aggregates, but there was also a large amount of open cracks in the aggregates and disaggregated particles. ASR gel was present in some of the open cracks in the aggregates and in a few cracks in the cement paste. While there is some cracking in the cement paste, most of the distress occurs in the aggregates. The fine aggregate in the concrete had the most disaggregated particles.

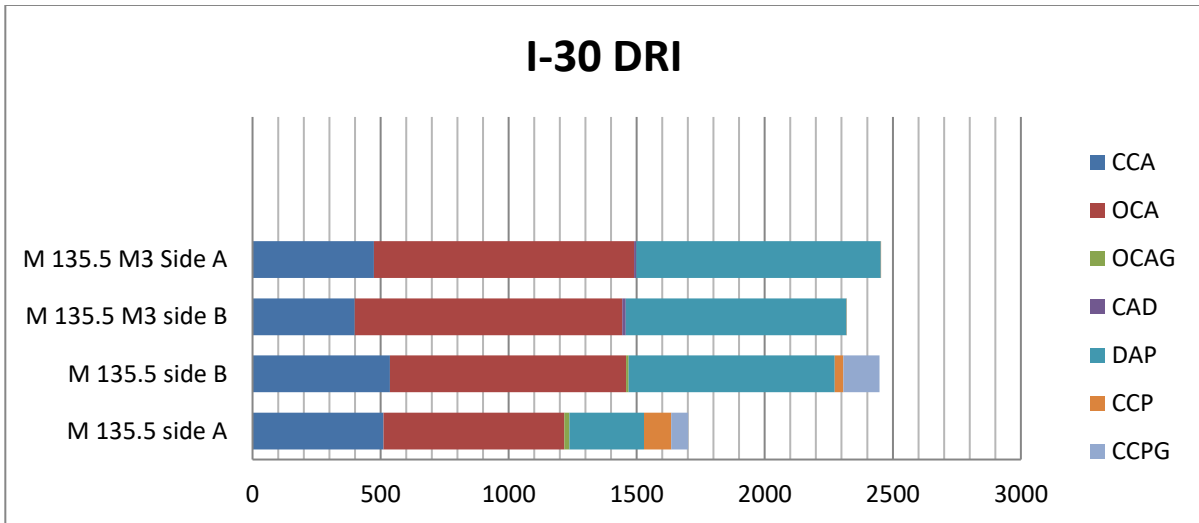


Figure 4.3. I-30 DRI

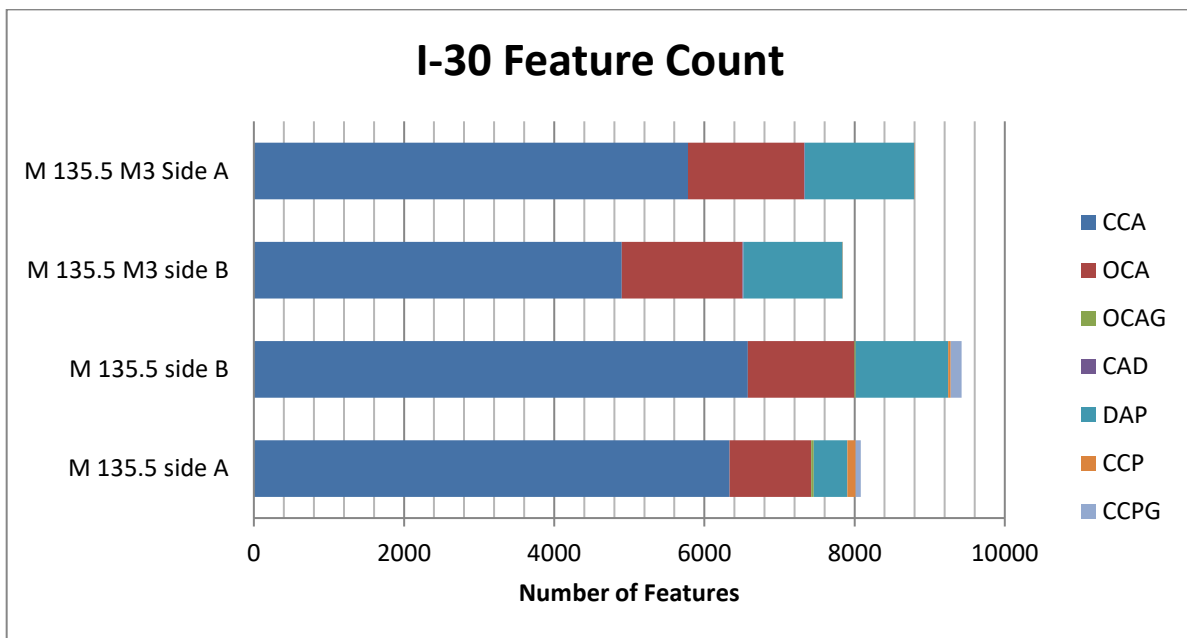


Figure 4.4. I-30 Feature Count

#### 4.2.3 I-49 Pavement:

In the summer of 2014, cores were taken from the I-49 pavement near Winslow, Arkansas. The pavement and barrier wall on I-49 had been experiencing map cracking and D-cracking. The DRI numbers and feature counts are given in Figure 4.5 and Figure 4.6, respectively. The I-49 pavement is slightly to moderately distress as exhibited by DRI numbers

ranging from 100-650. The main feature in the cores was closed cracks in the aggregate. In the slightly damaged cores (DRI 0-350), there was a small amount of open cracks in the aggregates and cracks in the cement paste. However, in the moderately damaged cores (DRI 350-600), there are some open cracks in the aggregates and cracks in the cement paste. ASR gel was present in each core, but it was in small quantities within the cracks or lining the inside of voids.

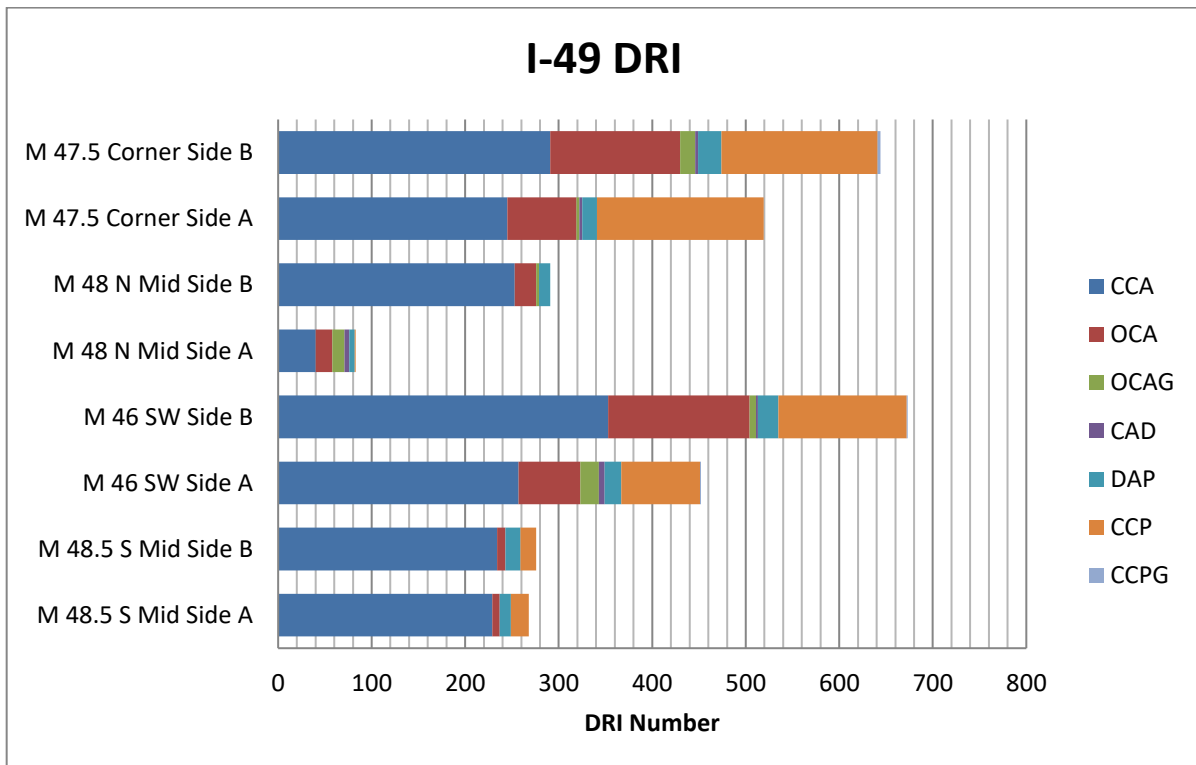


Figure 4.5. I-49 DRI



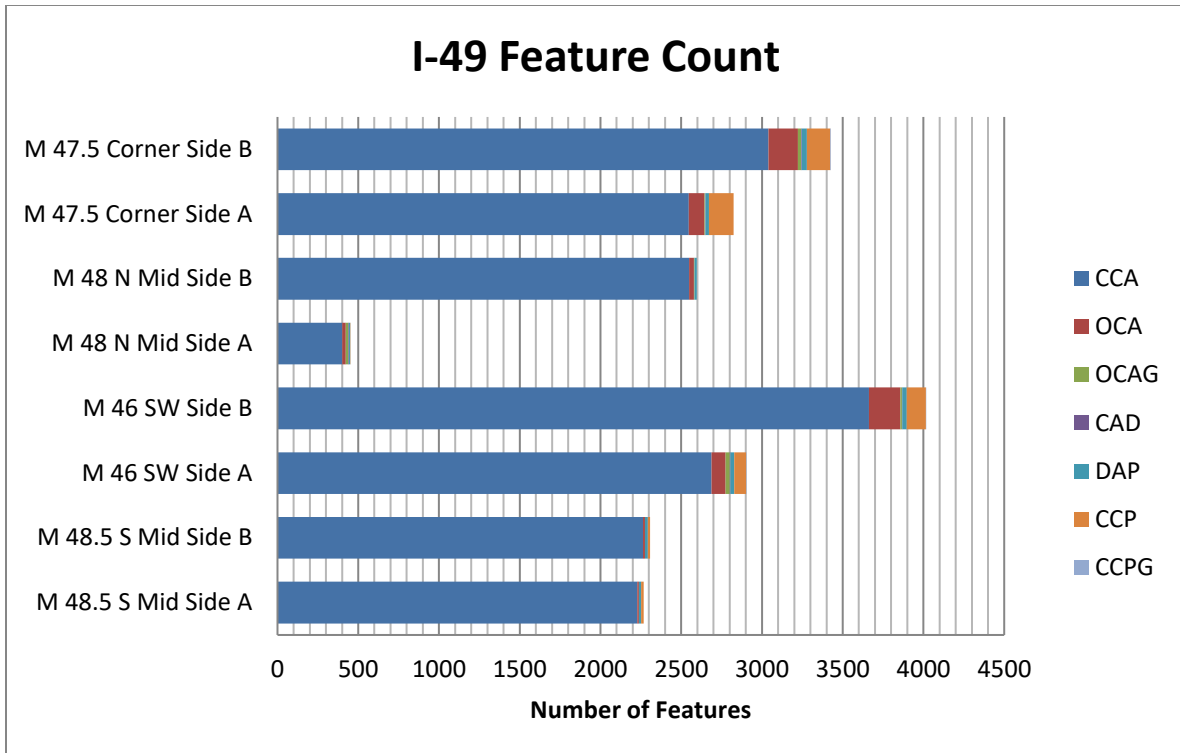


Figure 4.6. I-49 Feature Count

Cores, M 47.5 Corner and M 46 SW, had aggregates that appeared to have “exploded.” The aggregates were still intact and not disaggregated, but the inside of the aggregates had a large array of closed cracks. The damage could be from freeze-thaw within the aggregate. As ice forms, it would create hydraulic osmotic pressure within the aggregate causing the cracking of an “exploded aggregate as shown in Figure 4.7. It was unclear of how to classify these “exploded” aggregates. It was decided to count each crack as a closed crack.

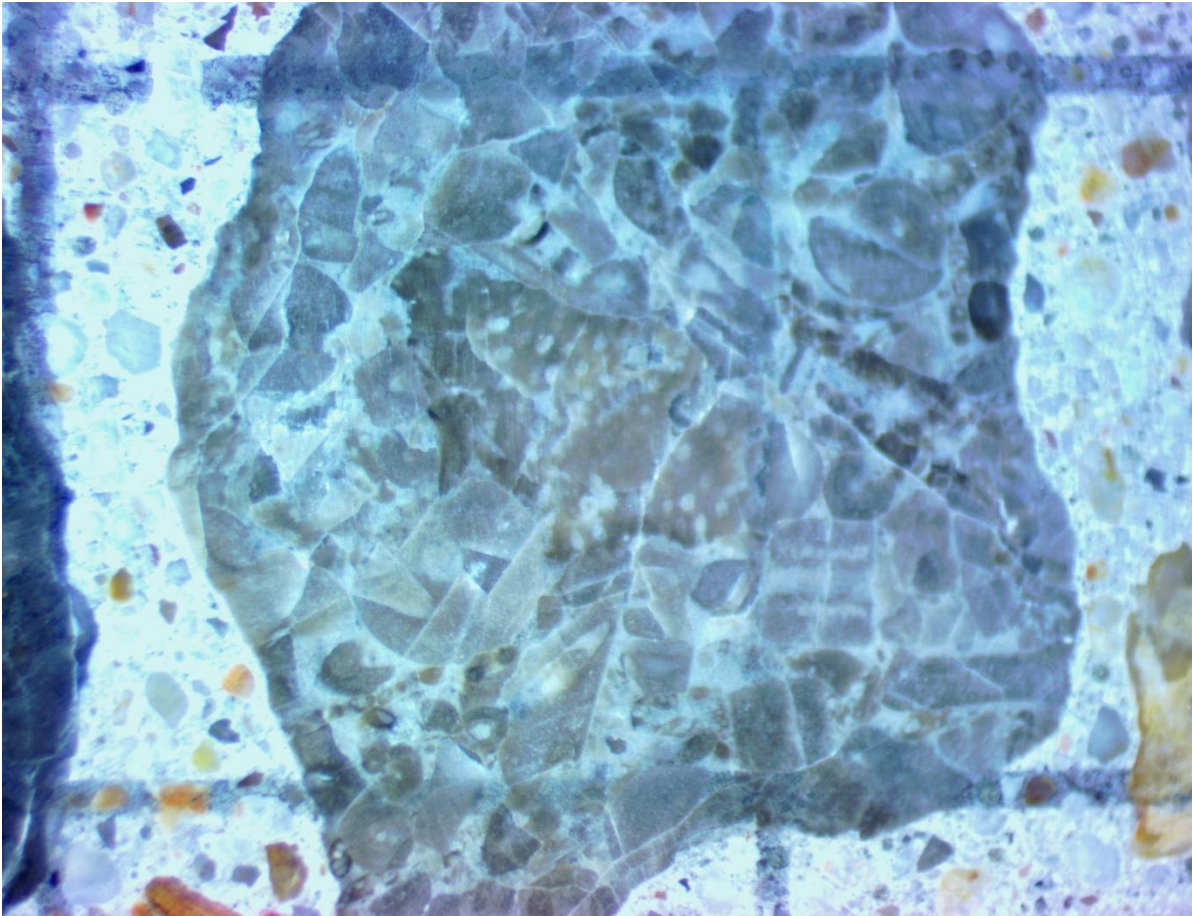


Figure 4.7. An “Exploded” Aggregate

#### 4.2.4 Joint and Mid Slab:

The location of the cores taken from I-530 in the spring of 2014 and I-49 in the summer of 2014 were known. The cores were either taken near the joints in the pavement slabs or from the middle of the slabs. Comparing their DRI numbers and feature counts in Figures 4.8-4.11, the cores taken near the middle of the slab had lower DRIs than those taken from the joints. The mid slab DRIs ranged from 80 to 450, which would mean that there is slight to moderate damage in the middle of the slabs. There is also slight to moderate damage in the joint cores because the DRI ranges from 200 to 650. The mid slab cores’ DRIs infer slight damage, while the joint cores’ DRIs tended to be moderate damage based on DRI number. The majority feature for both

mid slab and joint cores was closed cracks in the aggregates. The mid slab cores had little ASR gel, while the core joints had more ASR gel in the open cracks in aggregates. The cores from the joints also had more cracks in the cement paste and open cracks in the aggregates.

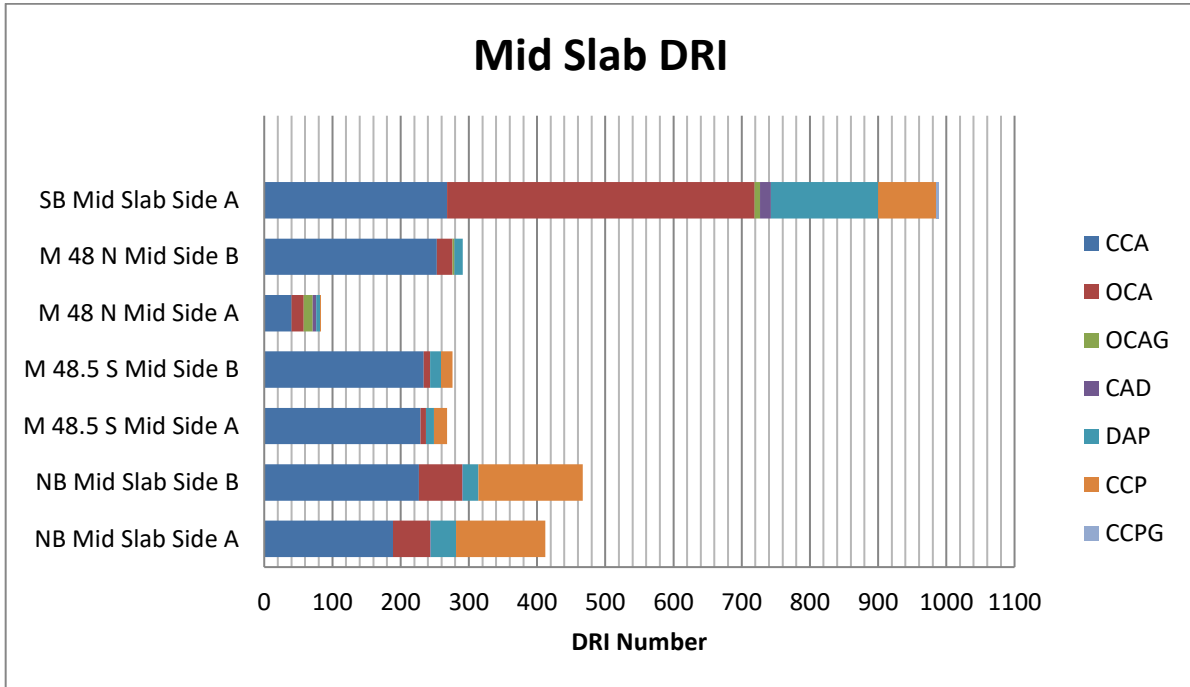


Figure 4.8. Mid Slab DRI

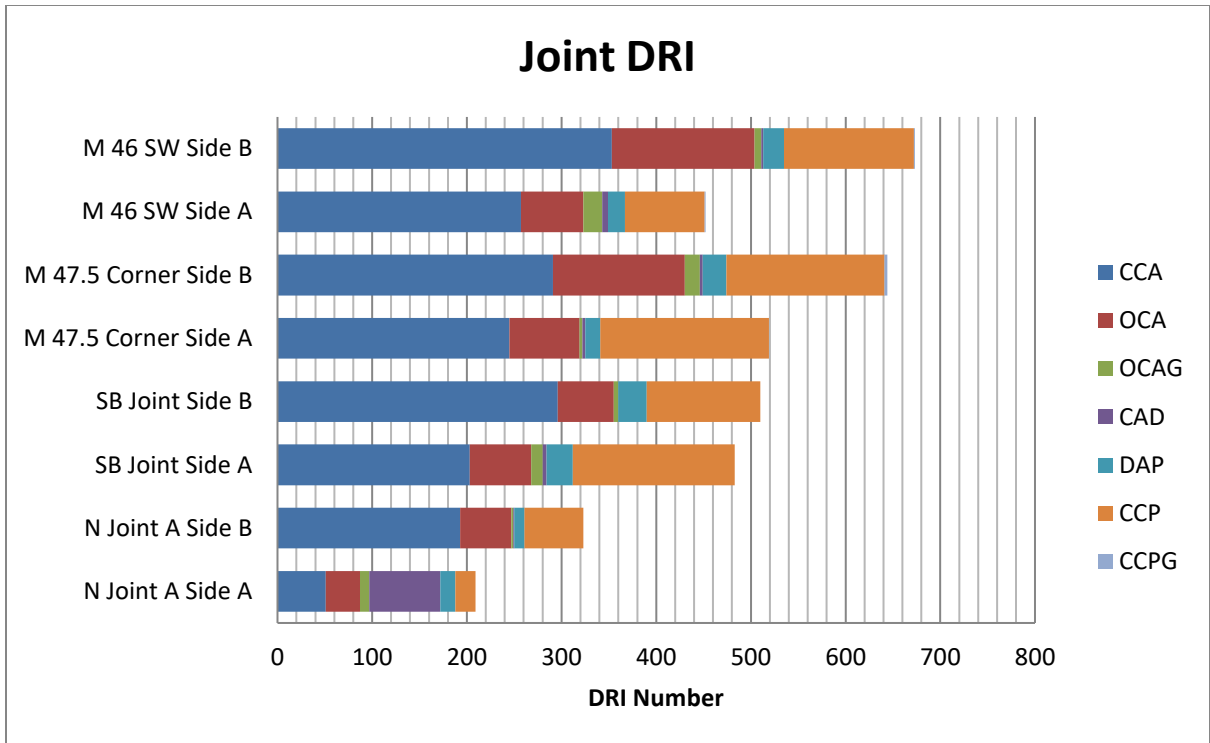


Figure 4.9. Joint DRI

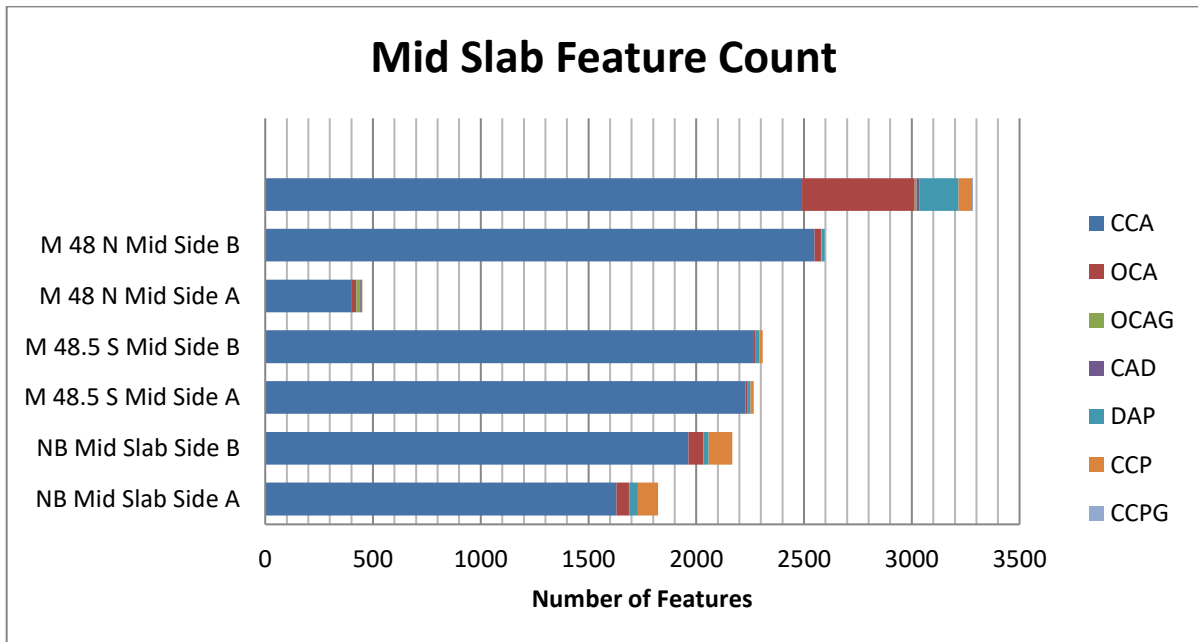


Figure 4.10. Mid Slab Feature Count

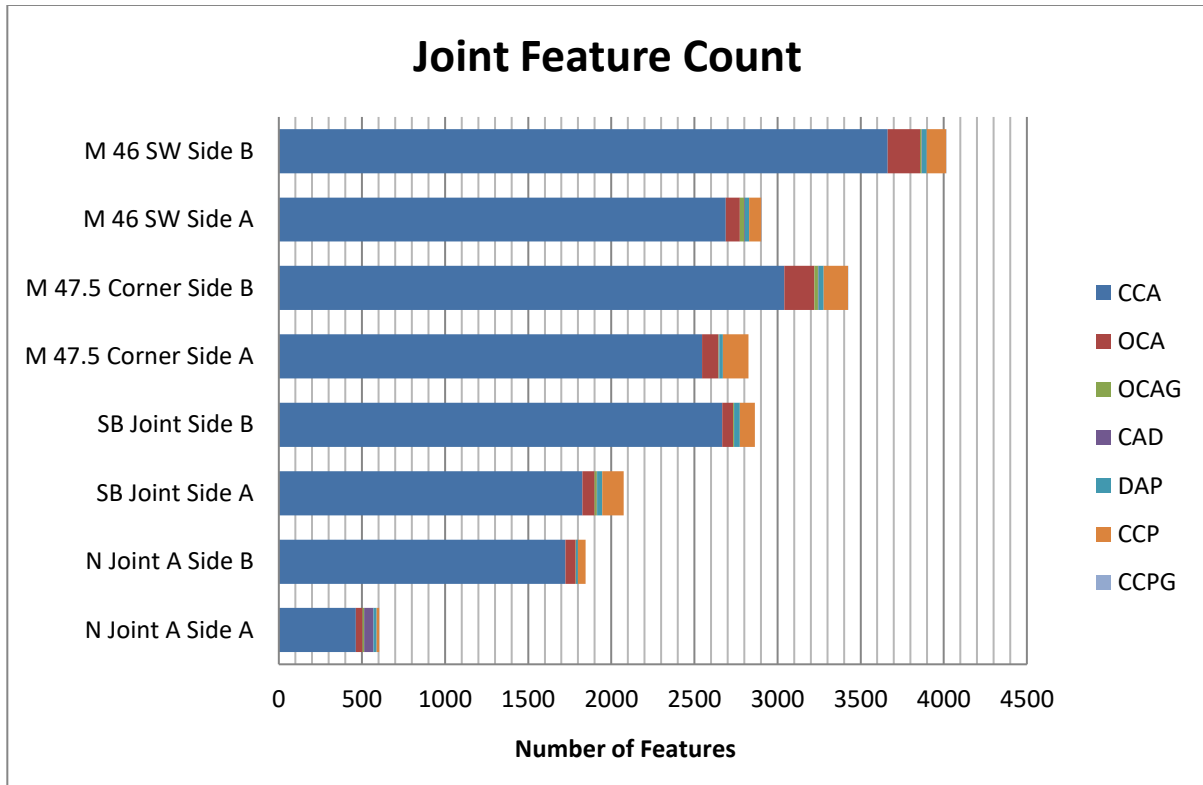


Figure 4.11. Joint Feature Count

#### 4.3 Potential for Further Expansion Test

In the summer of 2014, several cores were taken from the I-49 pavement. Nine of those cores were subjected to the Potential for Further Expansion Test (PFET). The PFET was previously described in Chapter 3. After one year of measurements, the strains were calculated for each set of cores and are presented in Figure 4.12.

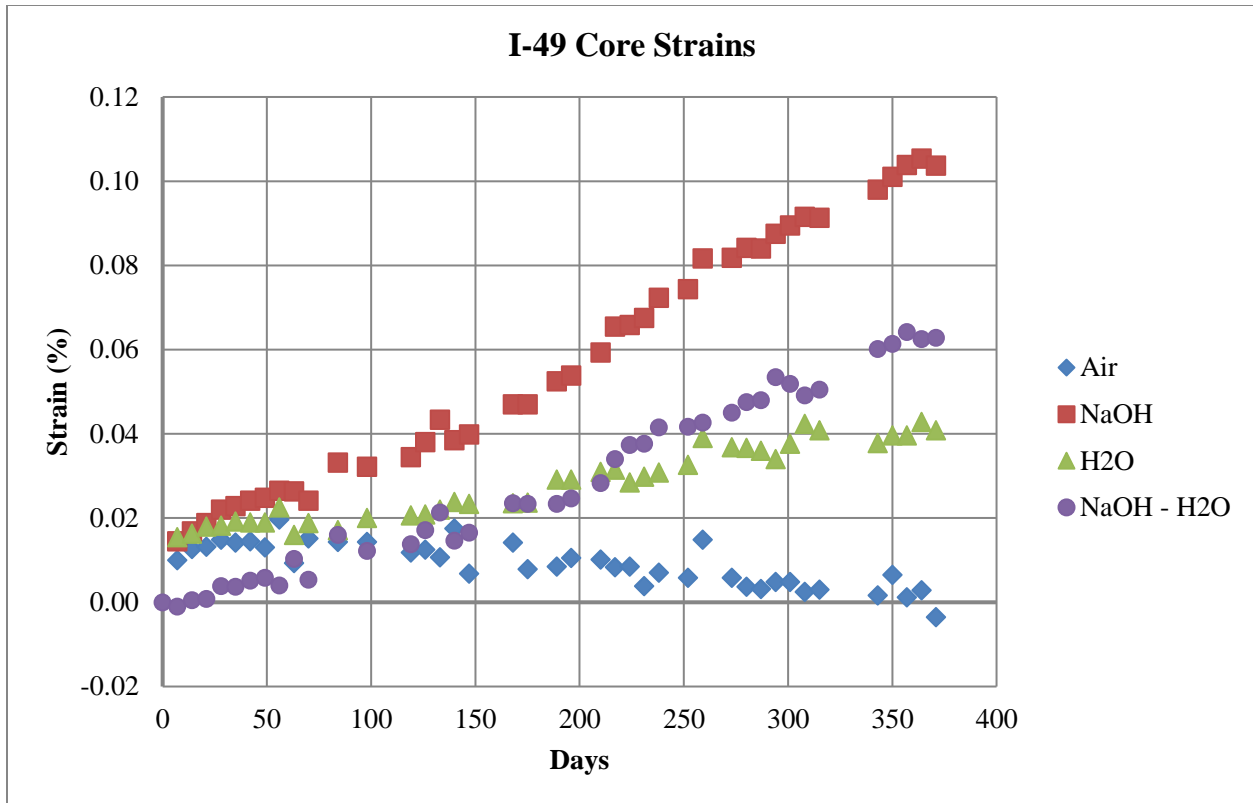


Figure 4.12. PFET on I-49

The set of cores submerged in 1N NaOH expanded over the course of the year. There is a slight decrease in the expansion just before six months, which indicates that the sodium in solution was being consumed by the cores to produce ASR gel. After a replacement of 1N NaOH, the reaction resumes which increases the rate of expansion. The expansion of the cores in NaOH indicates that there is still a sufficient supply of reactive silica in the concrete.

The cores that were submerged in water expanded throughout the testing, but not at the same rate of expansion that the cores in 1N NaOH exhibited. The cores stored in water expanded for a month and then the expansion leveled off. The leveling off was due to the cylinders reaching their absorption capacity. However, the cores in water expanded for the entire year. This points to the fact that there is already ASR gel within the concrete, and as that gel comes into contact with water, the cores expand allowing more water to be drawn in. The water cores were used to measure the amount of length change that occurs due to water absorption. By

subtracting the water cores' expansion from the NaOH cores' expansion, the resulting expansion due to ASR alone is slightly over 0.06 percent. This expansion is greater than the 0.03 percent limit for acceptable expansion, meaning there should be more expansion in the concrete.

The cores that were stored in air over 1 in of water contracted during the course of a year. If the air cores had expanded over the course of the year, then it would have shown that there was enough alkalis and reactive silica in the concrete to continue ASR. However since the air cores contracted over the year, there are not enough alkalis left in the concrete to produce ASR.

#### 4.4 ASR and Freeze-Thaw Mitigation by Sealers

In November 2014, the Group 1 blocks were cast. These blocks have been monitored for two years. The expansion results for each treatment are given in Figures 4.13-4.17. With gage studs in each of the four corners forming a square, strain measurements were taken twice per side. The two strain measurements were averaged together and the initial average strain along that side was subtracted from it. The difference was then divided by the length of the comparator and multiplied by 100% to obtain percent strain for that side. The percent strain for two sides was averaged together for the North-South (N-S) and East-West (E-W) directions. Based on the percent strain and time, the trends for each direction were calculated, and the overall expansions are included in Tables 4.3-4.5. The expansion of each treatment was compared to the expansion of the control blocks. The average expansion of the control blocks was subtracted from the expansion of the treated block. Then, it was divided by the average expansion of the controls and multiplied by 100 percent. The percent change is given in Table 4.6.

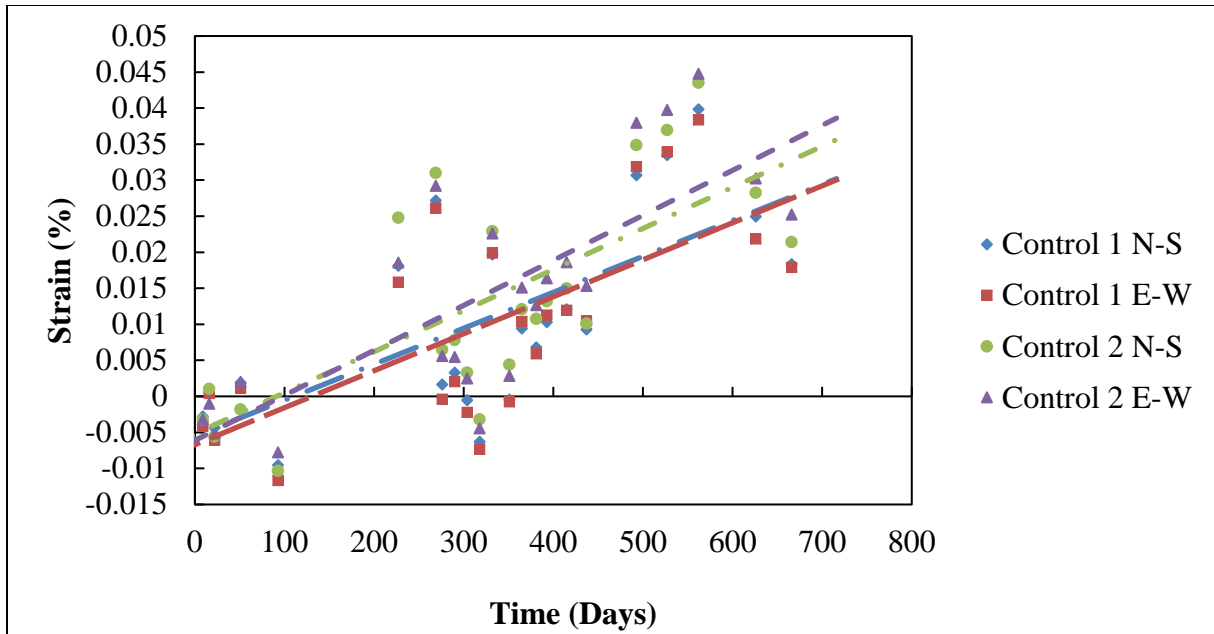


Figure 4.13. Control Blocks Strain Group 1

Table 4.3. Control Blocks Overall Expansion Group 1

Block	Percent Strain Expansion
Control 1 N-S	0.0333
Control 1 E-W	0.0333
Control 2 N-S	0.03996
Control 2 E-W	0.03996
Control Average	0.03663



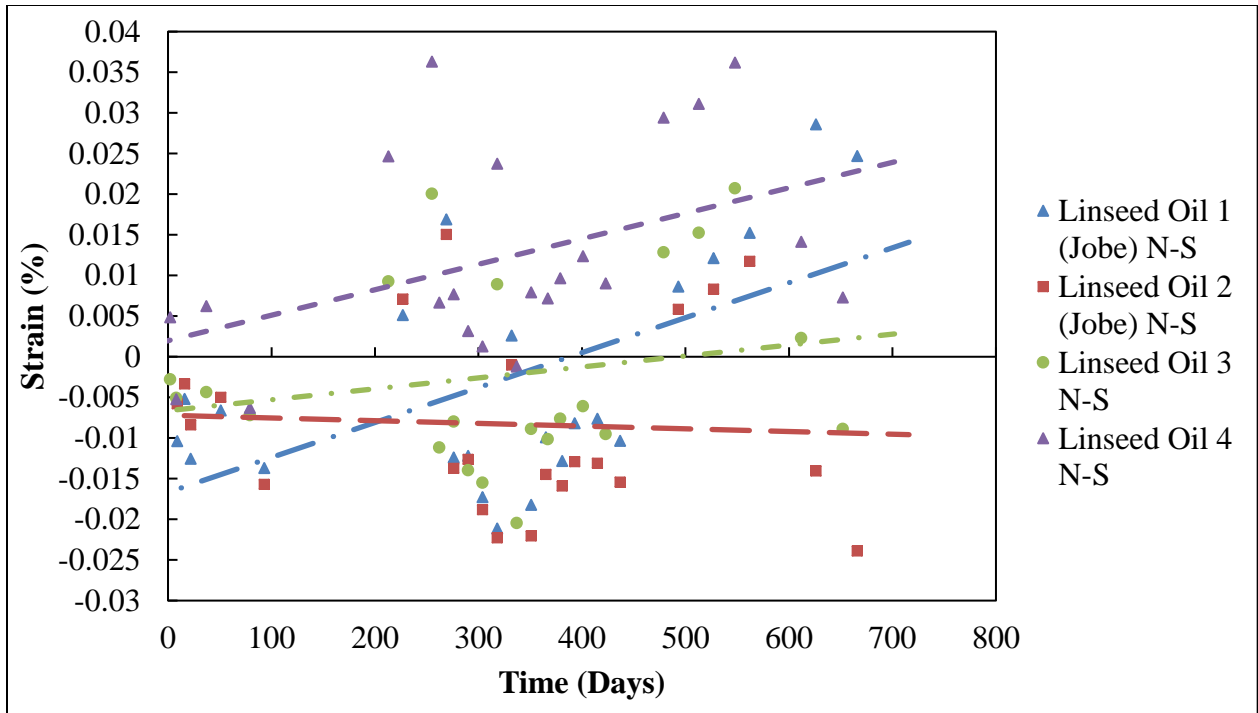


Figure 4.14. Linseed Oil Strain N-S Group 1

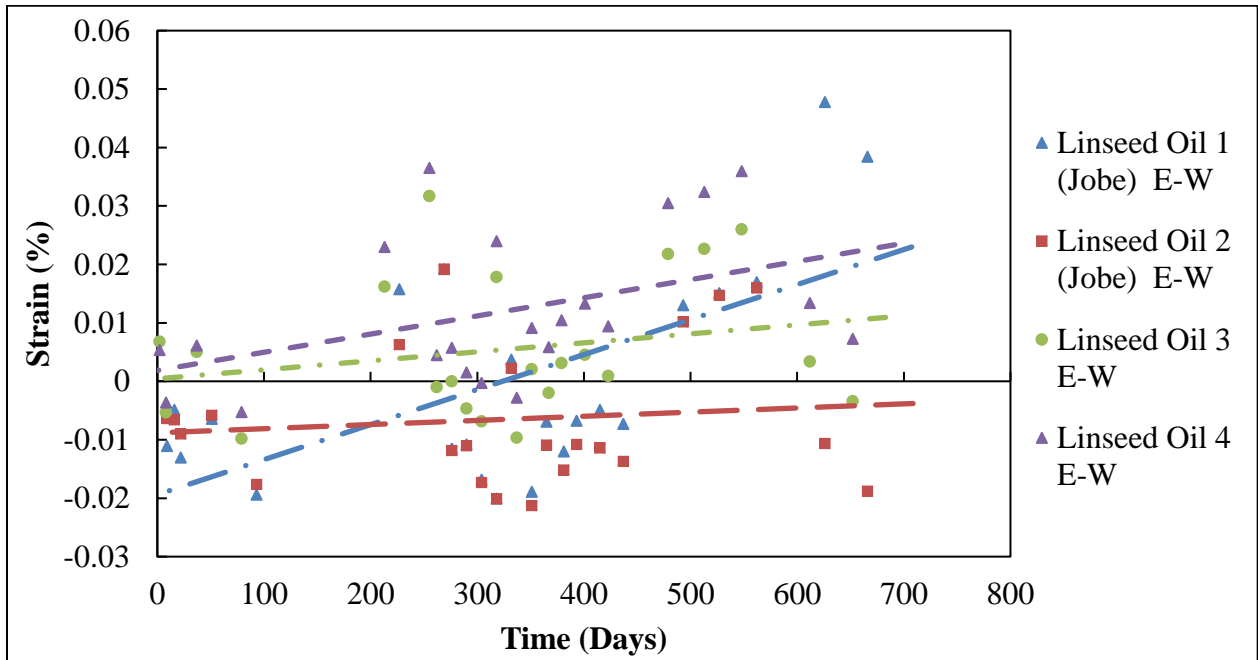


Figure 4.15. Linseed Oil Strain E-W Group 1

Table 4.4. Linseed Oil Overall Expansion Group 1

Block	Percent Strain Expansion		
	N-S	E-W	Average
Linseed Oil 1 (Jobe)	0.02664	0.03996	0.01732
Linseed Oil 2 (Jobe)	-0.002	0.00466	
Linseed Oil 3	0.0091	0.01304	0.01532
Linseed Oil 4	0.01956	0.01956	

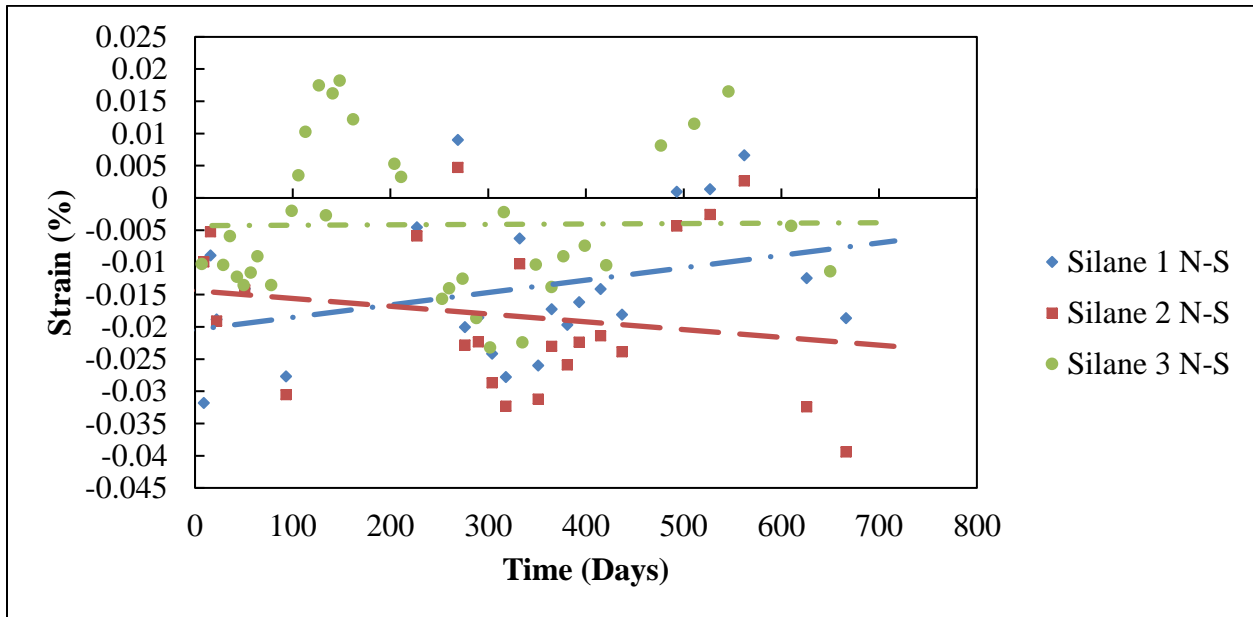


Figure 4.16. Silane Strain N-S Group 1

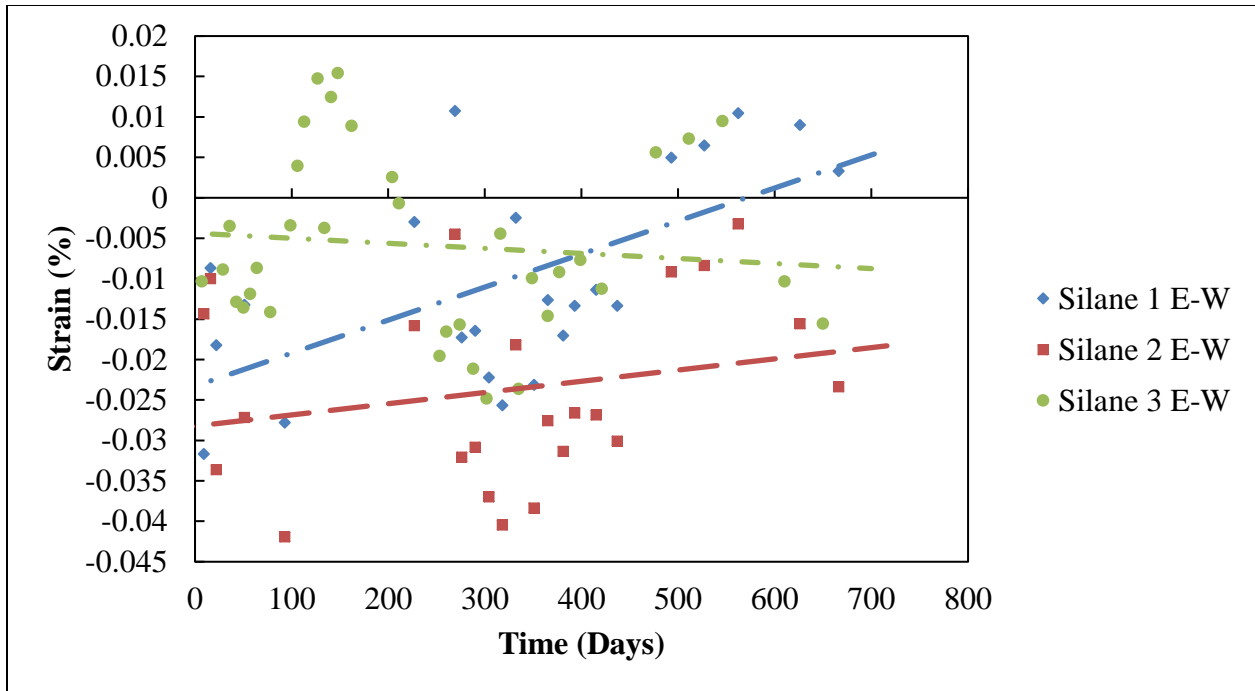


Figure 4.17. Silane Strain E-W Group 1

Table 4.5. Silane Overall Expansion Group 1

Block	Percent Strain Expansion		
	N-S	E-W	Average
Silane 1	0.01332	0.02664	0.006075
Silane 2	-0.00666	0.00666	
Silane 3	0.00039	-0.0039	

Table 4.6. Percent Change Group 1

Treatment	Change (%)
Linseed Oil (Jobe)	53
Linseed Oil	58
Silane	83

The expansion of the control blocks for Group 1 was 0.037%. Over two years all blocks expanded no matter the treatment. The Enviroseal silane reduced the amount of the expansion by 83 percent when compared to the control blocks. Both linseed oil treatments reduced the

amount by about 55%. The linseed oil block with Jobe sand expanded more than the linseed oil block without Jobe sand. This is to be expected because Jobe sand is more reactive than Arkansas River sand.

The Group 2 blocks were cast to determine a sealer to prevent ASR and freeze-thaw in concrete pavements. The blocks were measured at least once a month for 15 months. The expansion results are shown in Figures 4.18-4.23. The percent strain was calculated for each block in the N-S and E-W directions as it was done for Group 1 and are included in Tables 4.7-4.10. The percent change from the controls is shown in Table 4.11 and was calculated the same as Group 1.

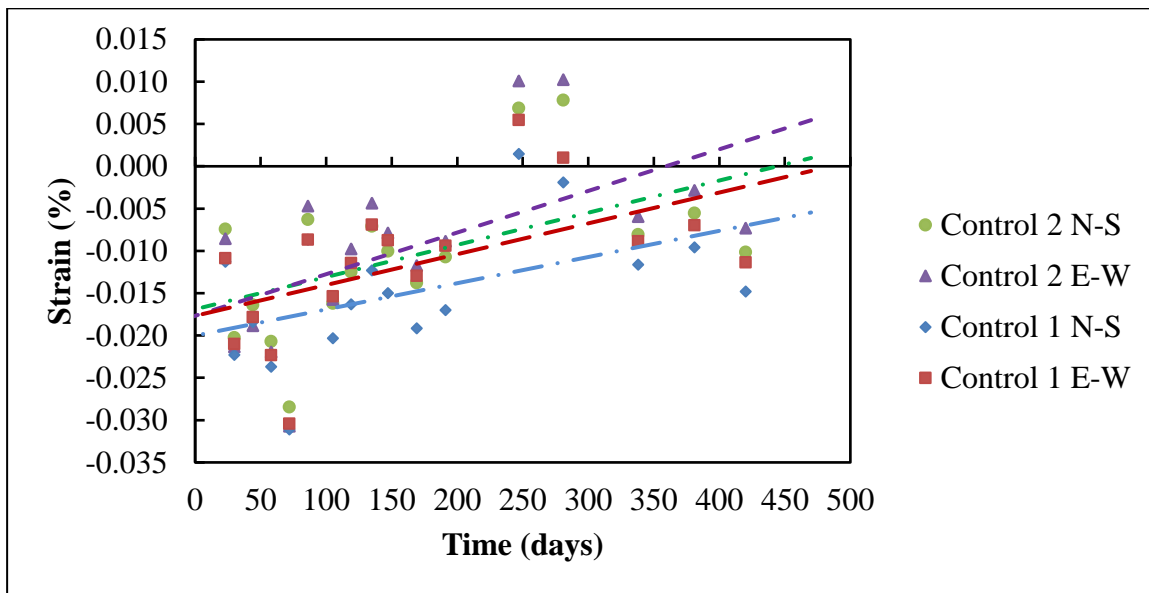


Figure 4.18. Control Blocks Strain Group 2

Table 4.7. Control Blocks Overall Expansion Group 2

Block	Percent Strain Expansion
Control 1 N-S	0.0126
Control 1 E-W	0.0168
Control 2 N-S	0.0168
Control 2 E-W	0.021
Control Average	0.0168

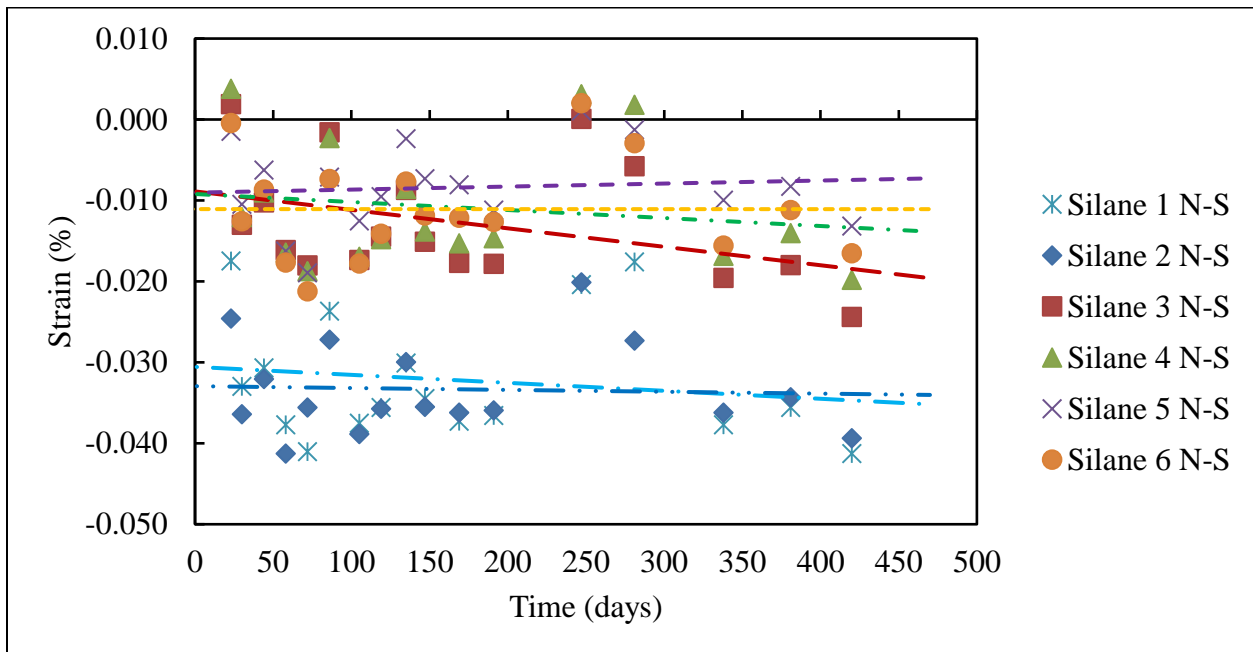


Figure 4.19. Silane Blocks Strain N-S Group 2

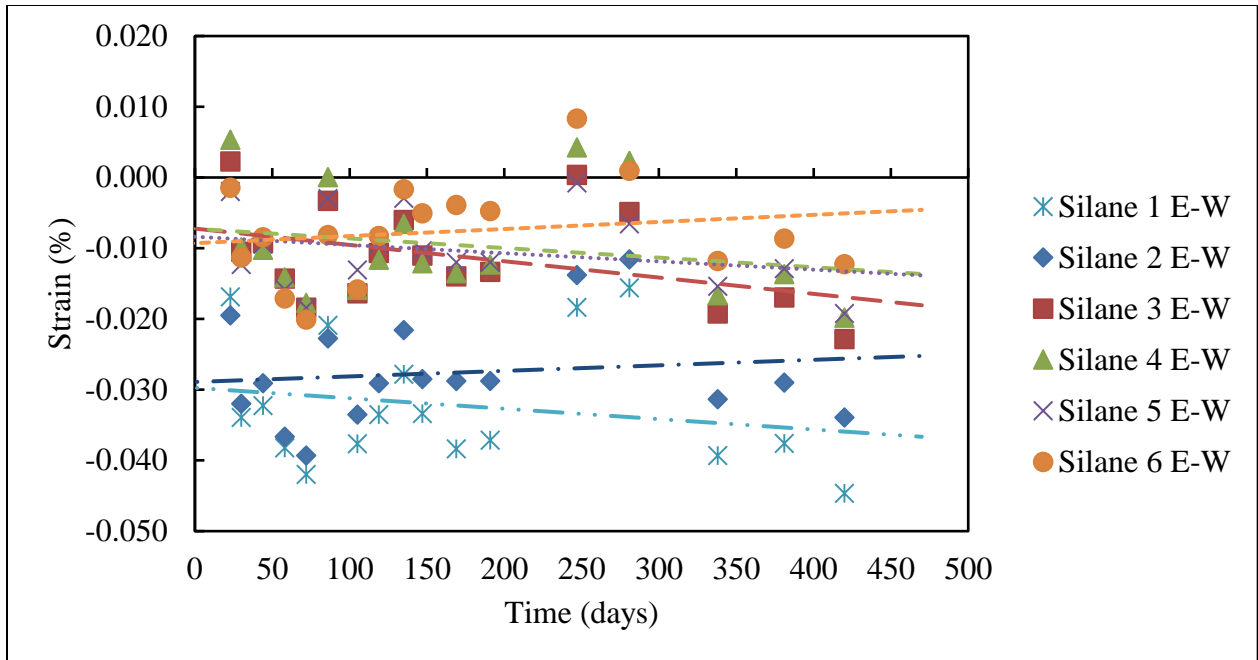


Figure 4.20. Silane Blocks Strain E-W Group 2

Table 4.8. Silane Blocks Overall Expansion Group 2

Block	Percent Strain Expansion		
	N-S	E-W	Average
Silane 1 (Enviroseal)	-0.0042	-0.0042	-0.00147
Silane 2 (Enviroseal)	-0.00084	0.00336	
Silane 3 (Sikagard)	-0.0084	-0.0084	-0.0063
Silane 4 (Sikagard)	-0.0042	-0.0042	
Silane 5 (Barricade)	0.00168	-0.0042	0.00042
Silane 6 (Barricade)	-0.0000042	0.0042	

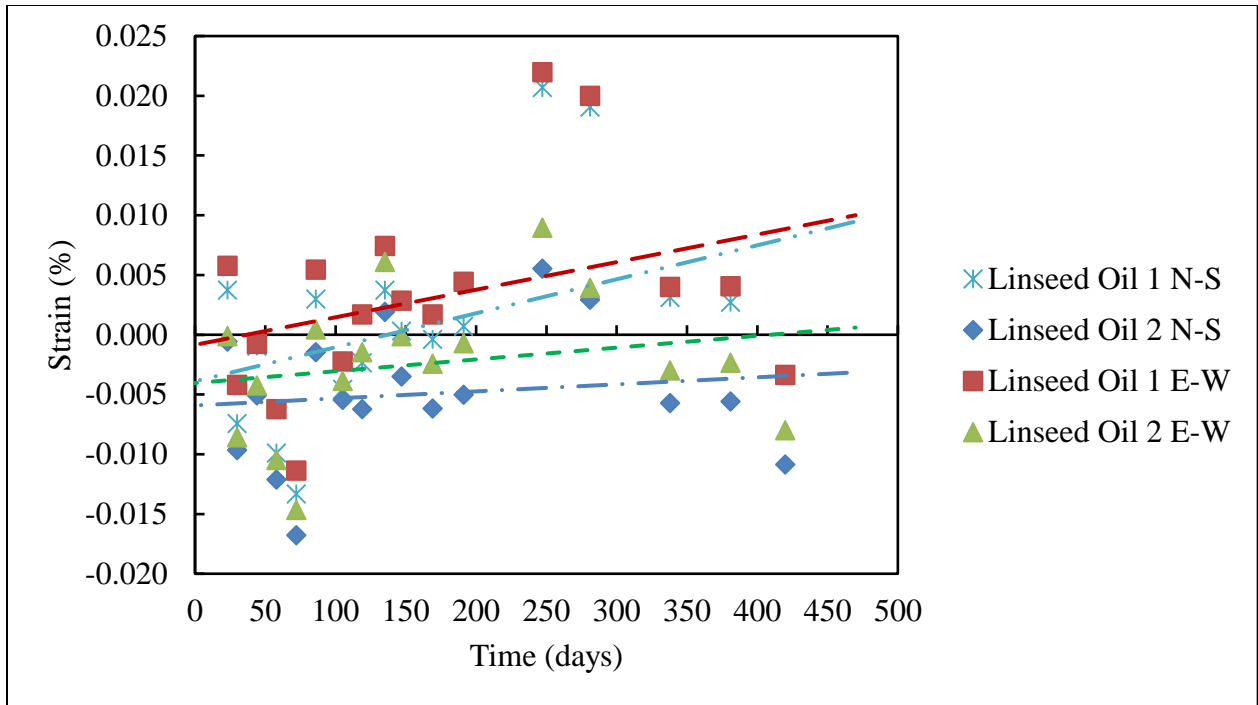


Figure 4.21. Linseed Oil Strain Group 2

Table 4.9. Linseed Oil Overall Expansion Group 2

Block	Percent Strain Expansion
Linseed Oil 1 N-S	0.0126
Linseed Oil 1 E-W	0.0084
Linseed Oil 2 N-S	0.00252
Linseed Oil 2 E-W	0.0042
Linseed Oil Average	0.00693

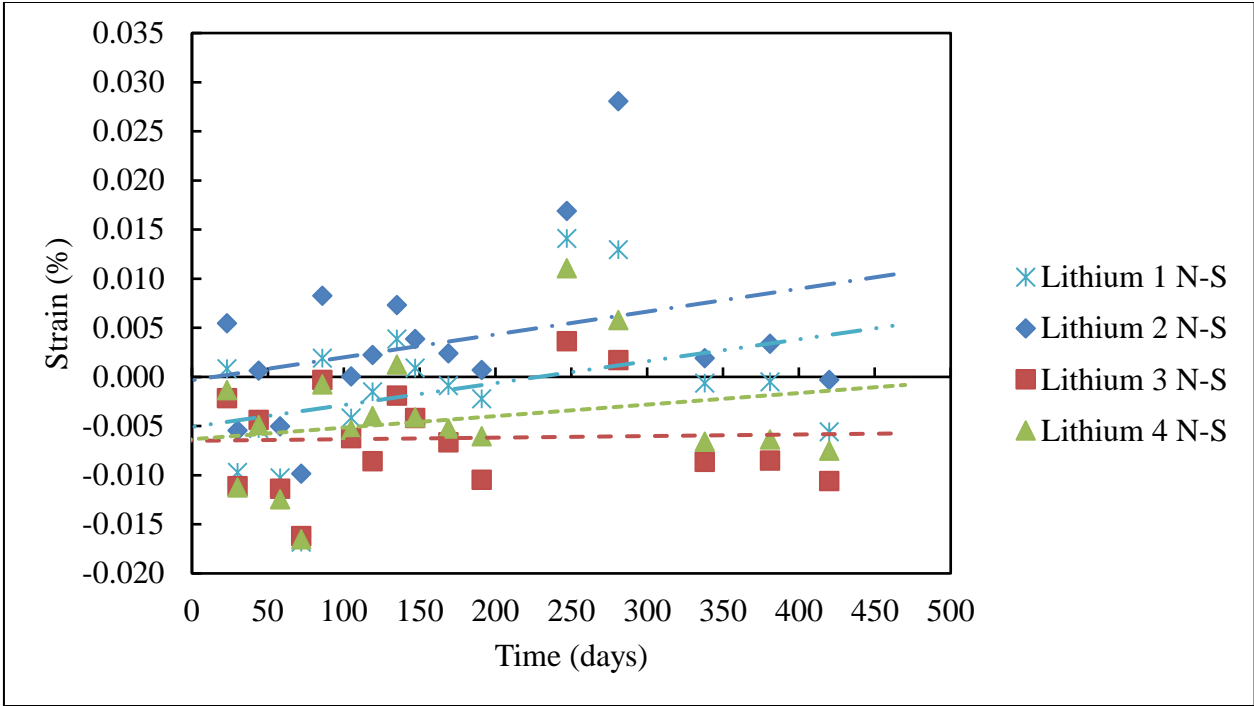


Figure 4.22. Lithium Strain N-S Group 2

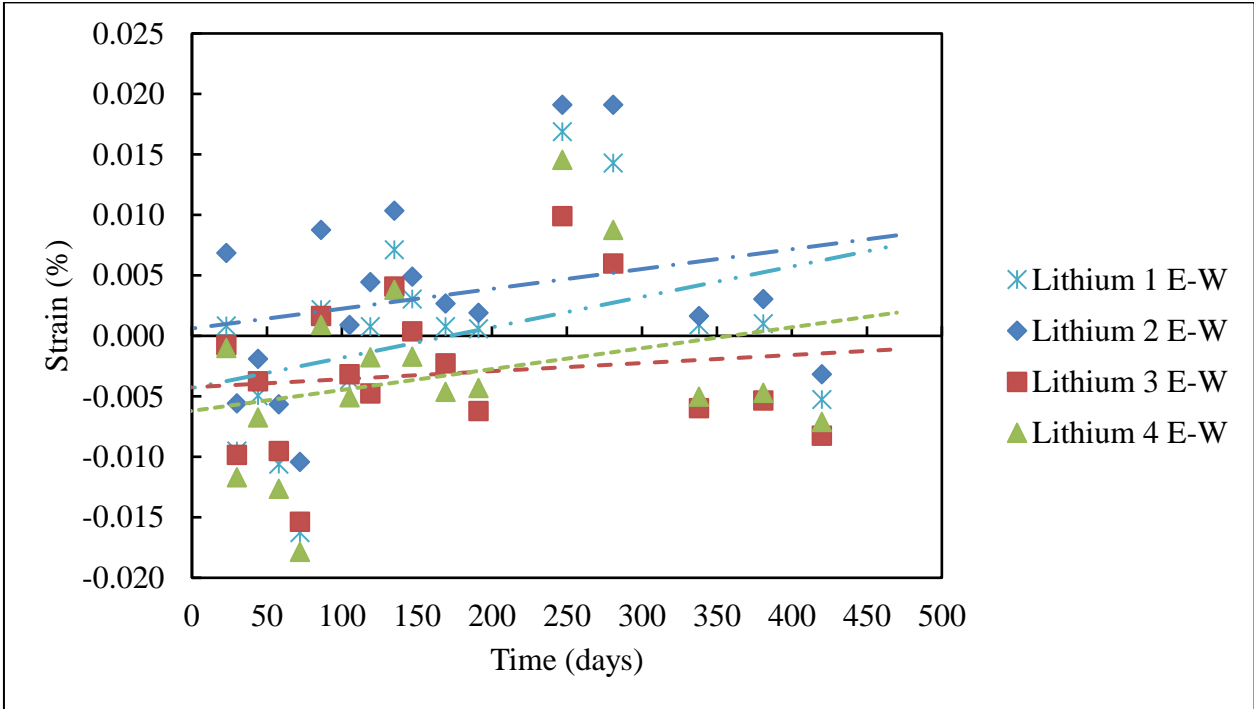


Figure 4.23. Lithium Strain E-W Group 2



Table 4.10. Lithium Overall Expansion Group 2

Block	Percent Strain Expansion		
	N-S	E-W	Average
Lithium 1 (double)	0.0084	0.0126	0.00945
Lithium 2 (double)	0.0084	0.0084	
Lithium 3 (single)	0.00084	0.00294	0.0041
Lithium 4 (single)	0.0042	0.0084	
Lithium Average	0.00677		

Table 4.11. Percent Change Group 2

Treatment	Change (%)
Enviroseal	109
Sikagard	138
Barricade	98
Linseed Oil	59
Lithium	60

The control blocks have expanded 0.017% since the beginning of the test. Both Enviroseal and Sikagard have contracted and not expanded over a year and three months. These treatments are 40% silane. Silanes have been known to cause shrinkage instead of expansion in the first 3-4 years after their application (Berube et. al. 2002). The Sikagard blocks have contracted more than those treated with Enviroseal and have the greatest percent change from the controls. The blocks treated with Barricade experienced slight expansion unlike the other silanes. Barricade is 100 percent silane. The linseed oil and lithium have expanded, but only to about 60 percent of the expansion that the control blocks experienced.

The lithium blocks sprayed a second time at one year have been expanding more than the lithium blocks only sprayed once. Both sets of blocks were cast using the same mix design and

sprayed at the same time at the beginning of the test. Even before Lithium 1 and Lithium 2 were sprayed a second time, they were still expanding more than Lithium 3 and Lithium 4. While everything between the blocks appears to be equal, their difference could be from the heterogeneous nature of concrete. Lithium 1 and Lithium 2's blocks may have sections inside the concrete that have a large concentration of alkalis causing ASR to form more readily in those areas increasing expansion. Also, due to the limited amount of data of three months for the lithium blocks sprayed twice, it was decided to average all the lithium blocks together.

The temperature of the concrete at depths of 1.5 in and 3 in was recorded from the end of November to the end of February during the winter of 2015-2016. Knowing that the temperature at which ice exerts enough pressure to exceed the tensile strength of concrete is based on the compressive strength of the concrete, it was determined that 27.25°F was cold enough for the ice to crack the concrete in freeze-thaw from Powers' equation from 1945 (Powers 1945). While no compressive strengths were taken of the concrete blocks, past experience with the aggregates used in a similar mix design yielded an average compressive strength of 7000 psi. The lows, duration, cooling rates, warming rates, and their averages were calculated for the days dropping below 27.25°F and are given in Tables 4.11-4.13.

Table 4.12. Concrete Temperature 1.5 in Below Surface

Day	Low (°F)	Duration (Min)	Cooling (°F/hr)	Warming (°F/hr)
01/02/2016	27.19	25.5	1.87	3.76
01/03/2016	24.35	347.5	1.78	9.81
01/05/2016	25.54	203.9	2.23	3.37
01/06/2016	23.83	419.3	2.07	7.81
01/11/2016	23.5	312.7	2.5	10.64
01/12/2016	19.87	752.9	2.03	8.96
01/14/2016	26.1	236.3	1.57	7.78
01/18/2016	22.82	458.7	1.87	7.43
01/19/2016	22.24	488.8	2.03	10.67
01/20/2016	26.15	194.6	1.24	2.79
01/28/2016	24.19	264.1	2.52	10.10
02/05/2016	24.84	217.8	2.61	10.76
02/06/2016	27.25	1	1.58	4.97
02/11/2016	25.63	271	2.39	7.78
02/27/2016	26.96	62.6	2.00	5.65

Table 4.13. Concrete Temperature 3 in Below Surface

Day	Low (°F)	Duration (Min)	Cooling (°F/hr)	Warming (°F/hr)
01/03/2016	26.89	113.5	1.28	4.41
01/06/2016	26.38	180.7	1.12	3.71
01/11/2016	26.46	132	1.94	4.82
01/12/2016	22.75	630.1	1.57	6.08
01/18/2016	25.63	275.5	1.67	3.94
01/19/2016	25.23	224.7	1.87	5.09
01/28/2016	27.18	48.7	1.66	4.41

Table 4.14. Average Concrete Temperature Data

Depth (in)	Average Low (°F)	Average Duration (Min)	Average Cooling (°F/hr)	Average Warming (°F/hr)
1.5	24.7	283.9	2.02	7.49
3	25.79	229.3	1.59	4.64

During the winter of 2015-2016, there were 15 times when the temperature dropped below 27.25°F at 1.5 in and 7 times at 3 in. This happened in January and February, which are on average the coldest months in Northwest Arkansas. The average low at 1.5 in was 24.7°F with an average duration below 27.25°F of 4 hr and 44 min. At 3 in the average low was 25.8°F with an average duration below 27.25°F of 3 hr and 49 min. It is apparent that the temperature of the concrete decreases more at the surface than the interior of the concrete. Also, the duration below 27.25°F decreases as depth increases. Both of these could be because concrete acts like an insulator, and it takes more time to cool the center of the concrete. The bottom of the blocks was

also in contact with the ground which would protect the bottom of the concrete from cold temperatures. Then as the sun rises and shines on the concrete, the block's temperature increases. With a warmer top and bottom, due to insulation, the center of the concrete heats up which shortens the duration and the low.

The warming rate at 1.5in is higher than the rate of warming at 3 in. This difference could just be the difference in depth because as the sun would rise in the mornings, the sun would hit the blocks' surfaces and quickly change the temperature at a shallow level of 1.5in. However, the interior of the block would still be colder and would take time to warm. This difference can be seen as the average rate of warming at 1.5in was 7.5°F/hr, while at 3in the rate of warming was 4.6°F/hr.

The rate of cooling was always lower than the rate of warming. This could once again be because of the sun. The sun hits the blocks in the morning, but by 2 pm in the afternoon the sun no longer is directly shining on the blocks because the blocks are being shaded by some trees. As the temperature would drop in the evening and into the night, the blocks would already be cooler and the rate of cooling would be less.

There were only trace amounts of precipitation on 3 of the times below 27.25°F (NOAA). The precipitation data obtained from NOAA can be found in Appendix A. With no actual precipitation to put 10% water into the cross-section, it is very unlikely that any damage was sustained below the surface, and that there were any freeze-thaw cycles. All damage would be experienced at the surface, most likely less than a quarter inch in depth. Such a small depth would provide plenty of room for water to escape ice expansion and for osmotic pressure to be at a minimum since there is little water. Also, any protective barriers like linseed oil and silane would be able to easily protect against such small amounts of water. However, there still would

be a chance of minor damage at the surface, but it would take multiple winters before there would be any significant break in the barrier.

Since trace amounts of moisture have been observed and their effects on the concrete slabs have been recorded. The next step in research would be to continue to monitor the blocks and wait for a harsher winter to examine the effects of long exposure to snow and ice.

## **5 Recommendations and Conclusions**

### **5.1 Recommendations and Conclusions for DRI**

The cores taken from I-530, I-30, and I-49 were all taken within one year of each other between the spring of 2014 and the spring of 2015. DRI was performed on all the cores. Overall, the major feature regardless of DRI number was closed cracks in the aggregates. ASR and freeze-thaw generally start in the aggregates as closed cracks. As the distress increases, these closed cracks open up and/or spread into the cement paste. Additionally, new closed cracks form in the aggregates. This was observed in cores. The visual inspection of the pavements ranged from slightly damaged (I-49) to severely damaged (I-30). The damage was reflected in the DRI number, and as the DRI number increased, the amount of open cracks and cement paste cracks increased. It is also noticeable in that the amount of features that were counted increased as the damage increased.

The DRI number is larger for cores taken from the joint of a slab, then those cores taken from the middle of the slab. The increase in DRI at the joint happens because there is already a pre-made crack in the concrete. Over time water, road debris, and deicing salts are forced into the saw-cut joint by traffic. Freeze-thaw causes the water to expand and crack the concrete around the joint. Water can then enter the concrete and repeated freeze-thaw cycles will cause D-cracking. These repeated freeze-thaw cycles can also lead to laminations throughout the top of concrete. This was seen in several of the cores taken from I-530. Deicing salts are known to contain alkalis, and as the concrete cracks, they penetrate into the concrete and react with siliceous aggregates to form ASR gel. As water also penetrates into the concrete and comes into contact with the gel, it expands causing more cracking. The combination effects of ASR and freeze-thaw at the joints produces a higher DRI number. It is recommended that the location of

the core in the slab be recorded along with a picture, so that the petrographer or examiner who performs DRI will know what damage to expect.

Several of the cores taken from I-49 had “exploded” aggregates. The cracking appears to be a uniform network of closed cracks throughout the aggregate. This shattered effect could be from water that froze inside the aggregate, which is likely because I-49 has been showing signs of D-cracking. The cracks in the aggregate will make the aggregate weaker and ultimately weaken the concrete, making this a feature of distress. The shape of the cracking lends itself to looking like a network of cracks which would be an OCA with a weight of 2. The extent of the cracking throughout the whole aggregate would be like a DAP with a weight of 2. It is recommended that a new feature be added to the DRI features list to include “exploded” or “shattered” aggregates. This feature would be used to help identify freeze-thaw distress and would carry a weight of 2. This weight factor would ensure that the number of cracks does not increase the DRI number when there are several “exploded” aggregates in a core.

## 5.2 Conclusions from the Potential for Further Expansion Test

The I-49 cores used for the Potential for Further Expansion Test (PFET) were test for one year. From the results, it is clear that the I-49 pavement will not continue to expand. The ASR gel that is already present inside the concrete will continue to expand and contract due to water slowly permeating into the concrete from rain. The water cores showed that there was existing ASR gel present in the concrete. The NaOH cores expanded due to the reactive silica of the aggregates, and the difference between the NaOH and water cores yielded an expansion of 0.06%, which is double the expansion that indicates further expansion. However, the air cores did not expand over the year but contracted. Therefore, there is not a sufficient amount of alkalis



left in the concrete to produce new ASR gel. With no new ASR gel, there will be no more expansion of the I-49 pavement.

It should be noted that due to the map cracking and D-cracking of the pavement, water will be able to permeate into the concrete. If this occurs during the winter months, there could be freeze-thaw damage. Also, if deicing salts or other alkali based compounds are used on the pavement surface, it is possible that they will penetrate into the concrete. The presence of alkalis will react with the silica and create new ASR gel. This will lead to more expansion of the pavement. It is recommended that the cracking be dealt with before freeze-thaw or ASR continues in the concrete.

### 5.3 Conclusions from Mitigation

With I-49 showing signs of ASR and freeze-thaw damage, Groups 1 and 2 were cast with reactive sands and additional alkalis to induce ASR in the concrete. They were then placed outside to experience freeze-thaw cycles. Three different topical treatments were used on the blocks, silanes, linseed oil, and lithium, to determine a treatment that could reduce ASR expansion and prevent freeze-thaw damage.

First, the treatment that is working the best to reduce expansion is silane. All the silanes tested are out-performing linseed oil and lithium. Within the silanes tested, the best silane to reduce expansion has been Sikagard; however, the performance of Enviroseal is similar. The difference between the two may be how they were manufactured, but since they are close together in reduction of expansion, it can be concluded that a 40% silane works best. If a 40% silane could not be used, then a 100% silane would work to reduce expansion. The 100% silane, Barricade, reduced expansion by almost 100%.

Second, topical lithium and linseed oil reduce expansion by about 60%. While this may keep the expansion of the concrete lower than it would be without either treatment, eventually the concrete will expand enough to cause cracking and deterioration. If they were applied to a new pavement, then either treatment might keep expansion low enough for the concrete to reach its service life.

Third, the number of freeze-thaw cycles experienced by the concrete blocks was approximately 15, but it is difficult to tell how much water was present in the concrete at the time of freezing. With only trace amounts of precipitation on the concrete, it is unlikely that any real damage was sustained by the concrete blocks.

Due to the limited amount of time that this test has been ongoing, the conclusions here for 1 year and 3 months may not be applicable for a longer amount of time. It is recommended that the blocks be measured for at least 7 years to come to an accurate conclusion of how each sealer performs over time. Expansion readings along with recording winter temperatures should continue to determine the freeze-thaw and ASR damage.

## 6 References

- ASTM C 1260 (2014). Standard Test Method for Potential Alkali Reactivity of Aggregates (Mortar-Bar Method). *ASTM International*. 100 Barr Harbor Drive, PO Box C700, West Conshohocken, PA 19428.
- ASTM C 1293 (2015). Standard Test Method for Determination of Length Change of Concrete Due to Alkali-Silica Reaction. *ASTM International*. 100 Barr Harbor Drive, PO Box C700, West Conshohocken, PA 19428.
- ASTM C 227 (2010). Standard Test Method for Potential Alkali Reactivity of Cement-Aggregate Combinations (Mortar-Bar Method). *ASTM International*. 100 Barr Harbor Drive, PO Box C700, West Conshohocken, PA 19428.
- ASTM C 33-16 (2016). Standard Specifications for Concrete Aggregates. *ASTM International*. 100 Barr Harbor Drive, PO Box C700, West Conshohocken, PA 19428.
- ASTM C 666 (2008). Standard Test Method for Resistance of Concrete to Rapid Freezing and Thawing. *ASTM International*. 100 Barr Harbor Drive, PO Box C700, West Conshohocken, PA 19428.
- ASTM C 88 (2013). Standard Test Method for Soundness of Aggregates by Use of Sodium Sulfate or Magnesium Sulfate. *ASTM International*. 100 Barr Harbor Drive, PO Box C700, West Conshohocken, PA 19428.
- BASF. MasterProtect H 400. *Technical Data Guide*. <https://assets.master-builders-solutions.basf.com/Shared%20Documents/EB%20Construction%20Chemicals%20-%20US/Construction%20Systems/Data%20Guides/MasterProtect/basf-masterprotect-h-400-tds.pdf>. July 19, 2016.
- Bérubé, M. A., Chouinard, D., Pigeon, M., Frenette, J., Rivest, M., & Vézina, D. (2002). Effectiveness of sealers in counteracting alkali-silica reaction in highway median barriers exposed to wetting and drying, freezing and thawing, and deicing salt. *Canadian Journal of Civil Engineering*, 29(2), 329-337.
- Committee, A. C. I. (1998). State-of-the-art report on alkali-aggregate reactivity (221.1 R-98). *American Concrete Institute, Farmington Hills, Michigan*.
- Deschenes, R. (2014). Mitigation of Alkali-Silica Reaction (ASR) in an Interstate Median Barrier. (Masters' Thesis Dissertation, University of Arkansas at Fayetteville).
- Durand, B. and Chen, H. (1991). Preventive Measures against Alkali-Aggregate Reactions. *Petrography and Alkali-Aggregate Reactivity: Course Manual*. March 12-14, 1991. Ottawa, Ontario. CANMET. Pp. 399-489.
- Euclid Chemical. Barricade Silane 100 C. *Guide Specification*. <http://www.euclidchemical.com/products/construction-products/penetrating-sealersliquid-densifiers/penetrating-sealers/baracade-silane-100c/>. December 2014.

- Euclid Chemical. Linseed Oil Treatment. *Safety Data Sheet*. [http://euclidchemical.com/fileshare/ProductFiles/msds/027\\_55\\_U.pdf](http://euclidchemical.com/fileshare/ProductFiles/msds/027_55_U.pdf). August 13, 2015.
- Folliard, K. J., Thomas, M. D., Fournier, B., Kurtis, K. E., & Ideker, J. H. (2006). Interim recommendations for the use of lithium to mitigate or prevent alkali-silica reaction (ASR) (No. FHWA-HRT-06-073).
- Fournier, B., Berube, M.A., Folliard, K., and Thomas, M. (2010). Report on the Diagnosis, Prognosis, and Mitigation of Alkali-Silica Reaction (ASR) in Transportation Structures. *FHWA-HIF-09-004*. January 2010.
- Gebhardt, R. F. (1994). "Survey of North American Portland Cements: 1994," *Cement, Concrete, and Aggregates*, V. 17, No. 2, Dec., pp. 145-189.
- Grattan-Bellew, P. E., & Danay, A. (1992, September). Comparison of laboratory and field evaluation of alkali-silica reaction in large dams. In *Proceedings of the First International Conference on Concrete Alkali-Aggregate Reactions in Hydroelectric Plants and Dams*.
- Henderson, G. L. (2006). Freeze-thaw resistance of concrete with marginal air content. *FHWA-HRT-06-117*. December 2006.
- Janssen, D. J., & Snyder, M. B. (1994). Resistance of concrete to freezing and thawing (No. SHRP-C-391). *National Research Council*. Washington, DC. June 1994
- LabJack Corporation. EI-1050 Digital Temperature/Humidity Probe. *EI-1050 Datasheet*. <https://labjack.com/support/datasheets/accessories/ei-1050>. 2016.
- Lute, R. D. (2008). *Evaluation of Coatings and Sealers for Mitigation of Alkali-Silica Reaction and/or Delayed Ettringite Formation* (Doctoral dissertation, University of Texas at Austin).
- McCoy, W. J., & Caldwell, A. G. (1951, May). New approach to inhibiting alkali-aggregate expansion. In *ACI Journal Proceedings* (Vol. 47, No. 5). ACI.
- NOAA. Record of Climatological Observations. *U.S. Department of Commerce, National Oceanic and Atmospheric Administration, National Environmental Satellite, Data, and Information Service*. Station: Fayetteville Drake Field, AR. December 2015-February 2016.
- Powers, T. C. (1955). Basic considerations pertaining to freezing-and-thawing tests. In *ASTM Proceedings*. Volume 55. Pp. 1132-1155
- Powers, T. C. (1975). Freezing effects in concrete. *ACI Special Publication*. Volume 47. Issue 1. Pp. 1-12.
- Powers, T.C. (1945). A Working Hypothesis for Further Studies of Frost Resistance of Concrete. *ACI Journal Proceedings*. Volume 41. Issue 1. January 1945. Pp. 245-272.
- Powers, T.C., and Helmuth, R.A. (1953). Theory of Volume Changes in Hardened Portland-Cement Paste During Freezing. *Highway Research Board Proceedings*. Volume 32. 1953. Pp. 285-297
- Sanchez, L. F. M. (2014). *Contribution to the assessment of damage in aging concrete infrastructures affected by alkali-aggregate reaction* (Doctoral dissertation, PhD thesis. Laval University, department of geology and geological engineering).

- Sika. Sikagard 740W. *Product Data Sheet*. <http://usa.sika.com/en/building-envelope/02a026/02a026sa02/02a026sa02600/02a026sa02601.html>. October 21, 2014.
- Sinak Corporation. Sinak LS-825. *Safety Data Sheet*. <http://sinakcorp.com/wordpress/wp-content/uploads/2015/11/ls-825-SDS.pdf>. August 20, 2015.
- Stanton, T. (1940). Expansion of Concrete through Reaction between Cement and Aggregate. *American society of Civil Engineers*. 1940. Pp. 1781-1811.
- Stark, D. (1991b). The Moisture Condition of Field Concrete Exhibiting Alkali-Silica Reactivity. *American Concrete Institute*. Volume 126. 1991. Pp 973-988
- Stark, D.C. (1991a) "How to Evaluate the State of Alkali-Silica Reactivity (ASR) in Concrete," *Aberdeen's Concrete Repair Digest*. Aug-Sept. pp.104-107
- Stokes, D. B., Pappas, J., Thomas, M. D. A., & Folliard, K. J. (2002). Field Cases Involving Treatment or Repair of ASR-affected Concrete Using Lithium. In Proceedings of the 6th CANMET/ACI International Conference on Durability of Concrete (pp. 631-642).
- Stokes, D.B., Wang, H.H., and Diamond, S., "A Lithium-Based Admixture for ASR Control That Does Not Increase the Pore Solution pH," *Proceedings of the Fifth CANMET/ACI International Conference on Superplasticizers and Other Chemical Admixtures in Concrete*, SP-173, 1997, pp.855-867.
- Thomas, M. D. (2001). The use of silica fume to control expansion due to alkali-aggregate reactivity in concrete: a review. *Materials Science of Concrete VI. American Ceramic Society, Inc, 735 Ceramic Place, Westerville, OH 43081, USA, 2001.*, 377-433.
- Thomas, M. D., Folliard, K. J., Fournier, B., Rivard, P., Drimalas, T., & Garber, S. I. (2013). *Methods for Evaluating and Treating ASR-Affected Structures: Results of Field Application and Demonstration Projects—Volume II: Details of Field Applications and Analysis* (No. FHWA-HIF-14-0003).
- Thomas, M. D., Fournier, B., Folliard, K. J., Ideker, J. H., & Resendez, Y. (2007). *The Use of Lithium to Prevent or Mitigate Alkali-Silica Reactions in Concrete Pavements and Structures* (No. FHWA-HRT-06-133).
- Thomas, M., Baxter, S., Stokes, D., & Hill, R. (2001). The combined use of fly ash and lithium nitrate for controlling expansion due to alkali-silica reaction. In *International Center for Aggregates Research 9th Annual Symposium: Aggregates-Concrete, Bases and Fines* (No. Final Draft).
- Villeneuve, V., Fournier, B., & Duchesne, J. (2012, May). Determination of the damage in concrete affected by ASR—the damage rating index (DRI). In *Proceedings of the 14th international conference on alkali-aggregate reaction in concrete, May* (pp. 20-25).
- Walker, H. N., Lane, D. S., & Stutzman, P. E. (2006). *Petrographic Methods of Examining Hardened Concrete: A Petrographic Manual. Revised 2004* (No. FHWA-HRT-04-150).
- Wright, J., Shen, Z., & Rizkalla, S. (1993). A three-year field and laboratory evaluation of linseed oil as a concrete sealer. *Canadian Journal of Civil Engineering*, 20(5), 844-854.

## Appendix A

### Record of Climatological Observations

These data are quality controlled and may not be identical to the original observations.  
 Generated on 09/29/2016

P r e l i m i n a r y	Y e a r	M o n t h	D a y	Temperature (F)		at O b s e r v a t i o n	Precipitation				Evaporation		Soil Temperature (F)							
				24 hrs. ending at observation time			24 Hour Amounts ending at observation time				At Obs Time	24 Hour Wind Movement (mi)	Amount of Evap. (in)	4 in depth			8 in depth			
				Max.	Min.		Rain, melted snow, etc. (in)	F i a g	Snow, ice pellets, hail (in)	F i a g	Snow, ice pellets, hail, ice on ground (in)			Ground Cover (see *)	Max.	Min.	Ground Cover (see *)	Max.	Min.	
	2016	1	1	42	21		0.00		0.0		0.0									
	2016	1	2	48	19		0.00		0.0		0.0									
	2016	1	3	48	22		0.00		0.0		0.0									
	2016	1	4	39	18		0.00		0.0		0.0									
	2016	1	5	45	17		0.00		0.0		0.0									
	2016	1	6	46	26		0.00		0.0		0.0									
	2016	1	7	50	43		0.14		0.0		0.0									
	2016	1	8	50	40		0.08		0.0		0.0									
	2016	1	9	40	21		0.15		T		0.0									
	2016	1	10	27	11		T		T		0.0									
	2016	1	11	43	14		0.00		0.0		0.0									
	2016	1	12	47	22		0.00		0.0		0.0									
	2016	1	13	56	20		0.00		0.0		0.0									
	2016	1	14	60	40		0.00		0.0		0.0									
	2016	1	15	52	28		0.00		0.0		0.0									
	2016	1	16	38	19		0.00		0.0		0.0									
	2016	1	17	32	16		T		T		0.0									
	2016	1	18	34	14		T		T		0.0									
	2016	1	19	37	21		0.04		T		0.0									
	2016	1	20	34	29		T		T		0.0									
	2016	1	21	36	27		0.10		T		0.0									
	2016	1	22	37	23		0.00		0.0		0.0									
	2016	1	23	43	24		0.00		0.0		0.0									
	2016	1	24	51	29		0.00		0.0		0.0									
	2016	1	25	61	36		0.00		0.0		0.0									
	2016	1	26	44	22		0.00		0.0		0.0									
	2016	1	27	50	16		0.00		0.0		0.0									
	2016	1	28	60	28		0.00		0.0		0.0									
	2016	1	29	69	25		0.00		0.0		0.0									
	2016	1	30	70	46		0.00		0.0		0.0									
	2016	1	31	68	38		0.00		0.0		0.0									
	Summary			47	25		0.51		0.0											

The "" flags in Preliminary indicate the data have not completed processing and quality control and may not be identical to the original observation  
 Empty, or blank, cells indicate that a data observation was not reported.  
 \*Ground Cover: 1=Grass; 2=Fallow; 3=Bare Ground; 4=Brome grass; 5=Sod; 6=Straw mulch; 7=Grass muck; 8=Bare muck; 0=Unknown "s" This data value failed one of NCDC's quality control tests.  
 "T" values in the Precipitation category above indicate a TRACE value was recorded.  
 "A" values in the Precipitation Flag or the Snow Flag column indicate a multiday total, accumulated since last measurement, is being used.  
 Data value inconsistency may be present due to rounding calculations during the conversion process from SI metric units to standard imperial units.

**Record of Climatological Observations**  
 These data are quality controlled and may not be identical to the original observations.  
 Generated on 09/29/2016

P r e l i m i n a r y	Y e a r	M o n t h	D a y	Temperature (F)		at O b s e r v a t i o n	Precipitation				Evaporation		Soil Temperature (F)							
				24 hrs. ending at observation time			24 Hour Amounts ending at observation time				At Obs Time	24 Hour Wind Movement (mi)	Amount of Evap. (in)	4 in depth			8 in depth			
				Max.	Min.		Rain, melted snow, etc. (in)	F l a g	Snow, ice pellets, hail (in)	F l a g	Snow, ice pellets, hail, ice on ground (in)			Ground Cover (see *)	Max.	Min.	Ground Cover (see *)	Max.	Min.	
	2016	2	1	64	33		0.00		0.0		0.0									
	2016	2	2	62	35		0.01		0.0		0.0									
	2016	2	3	42	22		0.00		0.0		0.0									
	2016	2	4	44	15		0.00		0.0		0.0									
	2016	2	5	51	20		0.00		0.0		0.0									
	2016	2	6	53	22		0.00		0.0		0.0									
	2016	2	7	53	27		0.00		0.0		0.0									
	2016	2	8	42	30		0.00		0.0		0.0									
	2016	2	9	40	23		0.00		0.0		0.0									
	2016	2	10	54	15		0.00		0.0		0.0									
	2016	2	11	58	26		0.00		0.0		0.0									
	2016	2	12	52	24		0.00		0.0		0.0									
	2016	2	13	50	27		0.00		0.0		0.0									
	2016	2	14	44	32		0.01		0.0		0.0									
	2016	2	15	58	32		0.00		0.0		0.0									
	2016	2	16	54	27		T		0.0		0.0									
	2016	2	17	62	23		0.00		0.0		0.0									
	2016	2	18	74	44		0.00		0.0		0.0									
	2016	2	19	71	50		0.00		0.0		0.0									
	2016	2	20	72	46		0.00		0.0		0.0									
	2016	2	21	70	48		T		0.0		0.0									
	2016	2	22	58	33		0.00		0.0		0.0									
	2016	2	23	45	32		0.55		T		T									
	2016	2	24	46	26		0.07		T		0.0									
	2016	2	25	43	24		0.00		0.0		0.0									
	2016	2	26	52	18		0.00		0.0		0.0									
	2016	2	27	68	36		0.00		0.0		0.0									
	2016	2	28	63	38		0.00		0.0		0.0									
	2016	2	29	68	27		0.00		0.0		0.0									
	Summary				56	29		0.64		0.0										

The "" flags in Preliminary indicate the data have not completed processing and quality control and may not be identical to the original observation. Empty, or blank, cells indicate that a data observation was not reported.  
 \*Ground Cover: 1=Grass; 2=Fallow; 3=Bare Ground; 4=Brome grass; 5=Sod; 6=Straw mulch; 7=Grass muck; 8=Bare muck; 0=Unknown "s" This data value failed one of NCEP's quality control tests.  
 "T" values in the Precipitation category above indicate a TRACE value was recorded.  
 "A" values in the Precipitation Flag or the Snow Flag column indicate a multiday total, accumulated since last measurement, is being used.  
 Data value inconsistency may be present due to rounding calculations during the conversion process from SI metric units to standard imperial units.